Utrecht University

Faculty of Geosciences

Copernicus Institute of Sustainable Development

Optimization of a multi-energy system associated to carbon-neutral hydrocarbon fuel synthesis

Author:
Janet Nienhuis

Supervisors:
Dr. Matteo Gazzani
Drs. Alexa Grimm
Drs. Lukas Weimann

August 4, 2019

Utrecht University

Abstract

A carbon-neutral alternative to fossil fuels is the synthesis of hydrocarbon fuels via the enhancement of carbon dioxide recovered from air, provided that the energy required to drive the separation is produced in a carbon-neutral way. The recovery of carbon dioxide from air and production of a synthetic fuel are both energy-intensive and complex processes. We investigated the conditions in which a system can be both carbon-neutral and economically feasible by looking at synthetic natural gas production via the Sabatier reaction enhancing one megaton of carbon dioxide per year, captured from air via a set of available technologies. Here, we build upon the modeling framework developed by *Gabrielli et al.*, which optimizes the multi-energy system using mixed integer linear programming, and resulting in selection, sizing, and scheduling of the technology portfolio to match a given synthetic natural gas profile. With this contribution we show how the optimal design of the energy system and its operation change upon varying conditions, such as electricity prices, carbon dioxide tax, weather data, and fuel production profile.

Keywords— carbon-neutral, DAC, hydrocarbon fuel synthesis, MES, DAC, PtG

Acknowledgements

This thesis reminded me that doing research starts with knowing nothing and ends with knowing I know nothing, yet learning so much. I would like to thank Matteo for all his time and support throughout the entire process. I really appreciate spending your vulnerable time on educating your students. Alexa, thank you so much for thinking along and keeping me sharp in times I got confused. Our weekly meetings stimulated me to get the best out of me and my research. Lukas, thank you for all your help on understanding and improving my knowledge of the tool. I can't wait to put my knowledge into practice and make the world a little greener.

To all of you, *Grazie mille* and *vielen Dank*.

Janet Nienhuis

Utrecht, August 2019

Contents

List of Figures

List of Tables

Nomenclature

ALKEC	Alkaline Electrolyzer Cell
CAPEX	Capital Expenditure
CE	Carbon Engineering
CW	ClimeWorks
DAC	Direct Air Capture
eHUB	energy HUB
FP	Fuel Production
GHI	Global Horizontal Irradiance
HOS	Hydrogen Oxygen Storage
HT	High Temperature
LHV	Lower Heating Value
LT	Low Temperature
MES	Multi Energy System
MILP	Mixed Integer Linear Programming
OPEX	Operational Expenditure
PEMEC	Proton Exchange Membrane Electrolyzer Cell
PEMFC	Proton Exchange Membrane Fuel Cell

PtG	Power to Gas
PV	Photovoltaic
RES	Renewable Energy Source
RWGS	Reversed Water Gas Shift
SNG	Synthetic Natural Gas
SOEC	Solid Oxide Electrolyzer Cell
SOEFC	Solid Oxide Fuel Cell
ST	Solar Thermal
UAE	United Arab Emirates
USA	United States of America
UU	Utrecht University
WGS	Water Gas Shift
WT	Wind Turbine

Chapter 1

Introduction

One of the biggest technical challenges society is facing in its endeavor to meet the goals set by the Paris Agreement is the decarbonization of heavy industry and the maritime and aviation transportation sector [2]. While renewable energy sources can substitute fossil fuels for electricity generation and household energy demands, the heavy industry and maritime and aviation transportation sector will likely stay in need of energy-dense hydrocarbon fuels [2]. A carbon-neutral alternative is the synthesis of such fuels via enhancement of CO_2 recovered from air, provided that the energy required to drive the separation is produced in a carbon-neutral way.

One way of producing a synthetic hydrocarbon fuel is via hydrogenation - a chemical reaction between hydrogen and another molecular compound. Carbon dioxide (CO_2) is one of the compounds that can be used to chemically react with hydrogen (H_2) to produce a fuel. The conversion of CO_2 and H_2 into a synthetic hydrocarbon fuel potentially kills two birds with one stone: reducing greenhouse gas emissions - by capturing CO_2 from flue gases, large CO_2 point sources or air - and increasing hydrocarbon fuel availability.

Hydrocarbon fuel synthesis is challenging because CO_2 on its own does not contain energy and needs to be recovered from ambient air using renewable energy sources (RES) to meet carbon-neutrality. On top of this is the dilute presence of CO_2 in ambient air of approximately 400 ppm complicating the process and makes the recovering process energy-intensive [3]. In addition is there the prerequisite that the second prime component, H_2, is produced in a carbon-neutral way as well as fuel synthesis.

Although the process of recovering CO_2 from ambient air was commercialized over 50 years

ago [3], synthetic fuel production is already being applied on small scale [4], and research has been conducted on both the technical and economical aspects of the process [3] [4], an optimization of the technologies involved in carbon-neutral hydrocarbon fuel synthesis is lacking.

1.1 Research Goal

Here, our aim is to investigate the energy system that supplies energy to the key processes, i.e. CO_2 recovery from air and hydrocarbon fuel synthesis and study the conditions in which the system can be carbon-neutral and economically feasible. This includes the level of interaction between the CO_2 recovery technology, fuel production technology, and between the multiple energy sources, carriers, and conversion and storage technologies. The trade off between excess renewable electricity as (i) an energy source for CO_2 capture or (ii) used for other energy conversion and storage technologies within an energy system will provide insight in the optimal design of a carbon-neutral synthetic fuel production system.

This work builds upon the modeling framework developed by [5], which optimizes multi-energy system (MES) using mixed integer linear programming (MILP), and intends to answer: *What is the optimal design, in terms of CO_2 emissions and costs, of a MES providing energy to a carbon-neutral synthetic hydrocarbon fuel production system?*

This report is structured by describing the components of the MES in Chapter 2 followed by presenting the optimization process of the MILP in Chapter 3. Chapter 4 describes the input data required for the optimization problem and the case study matching different operation modes and geographic locations. The results are presented in Chapter 5 followed by a discussion and conclusion in Chapter 6 and 7, respectively.

Chapter 2

Theoretical Framework

The type of energy source, energy carrier, moment of generation (supply and demand), and facility location is decisive for the decision on synthetic hydrocarbon fuel production. The origin of the electrical and thermal energy required for the fuel plays an important role in the economic and environmental feasibility. Since the production of synthetic hydrocarbon fuels is an energy intensive process [3] [6] [7], the utilization of renewable energy sources (RES) is essential as the integration of RES within the current energy system is essential for the realization of a carbon-neutral society. Synthetic hydrocarbon fuels can either be produced using RES within a centralized energy system or interconnected in a decentralized system, i.e. MES. The shift from a centralized energy system, consisting of the predictable behavior of conventional energy sources, to a decentralized energy system is required to cope with the intermittent behavior of RES [8]. A decentralized energy system entails both more integrated energy markets and infrastructures, such as electricity, gas, and water (thermal). Decentralized renewable electricity generation technologies, like photovoltaics and wind turbines, already plays a small role in the Dutch energy mix [9] and is expected to grow exponentially within the coming decades [10]. Different energy conversion technologies need to interact to match supply and demand, while keeping costs low. Hence, to successfully implement a decentralized energy system and optimally utilize the interaction between different energy sources, carriers, and conversion and storage technologies, the adoption of a MES is essential.

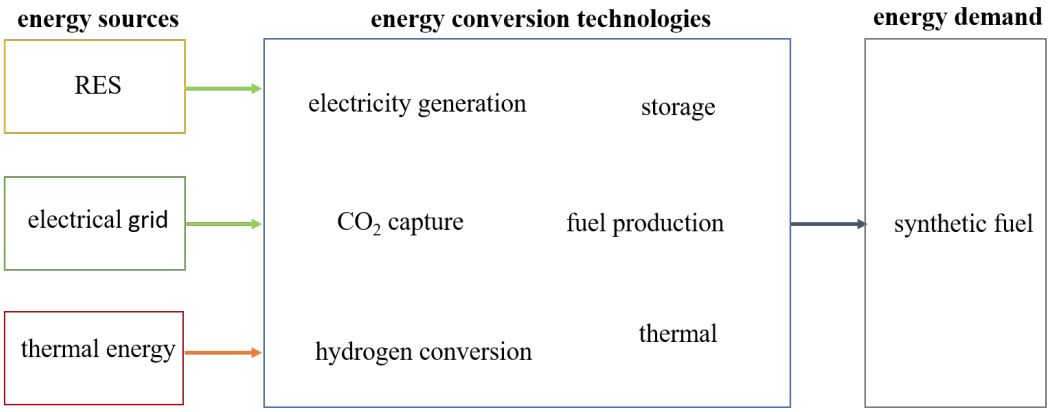

Figure 2.1: Simplistic representation of a multi energy system.

2.1 Multi Energy System

A MES combines energy sources, energy carriers, and conversion and storage technologies within a defined boundary (Figure 2.1). The level of interaction between the available technologies determines the complexity of the system. The number of technologies that can be combined, the different operation modes that can be adopted, the uncertainty of supply and demand, and the topology of MES integrated with the distribution grids makes implementation challenging [5].

The technologies that play a key role in the synthetic hydrocarbon fuel production system comprise the carbon dioxide sequestration technology and the fuel synthesis technology. The technical and economical characteristics of both technologies are addressed below.

2.1.1 Direct Air Capture

Direct air capture (DAC) is a collective name for all capture techniques that extract CO_2 directly from the atmosphere [11]. DAC differs from pre-, post- and oxy-combustion techniques in the way that the net CO_2-emission is negative - provided that the electrical and thermal energy demand comes from RES and the CO_2 is stored -, whereas the net CO_2-emissions in the latter techniques in most cases involves the combustion of carbon-based fossil fuels. As a result of the combustion of carbon-based fossil fuels the atmospheric CO_2-concentration has been increasing up until a current CO_2-concentration of 400 ppm [6]. This concentration is a factor 300 more dilute than the CO_2-concentration in flue gases from fossil fuel combustion [12], contributing to a significant energy demand per metric ton of CO_2 captured [11].

Technical aspects. In a DAC system ambient air flows through a contactor where CO_2 is chemically removed using a selective sorbent. The two most applied and researched recovery technologies are based on liquid sorbents, i.e. high temperature (HT) absorption, and solid sorbents, i.e. low temperature (LT) adsorption [3] [13]. At the end of the process most CO_2 (typically ranging from a 80 to 99 % CO_2-capture [3]) is removed from the stream and the CO_2-depleted air is released back to the atmosphere. The concentrated CO_2 stream is compressed and stored or transported for further use [11] [14].

The complete absorption and regeneration cycle typically involves four consecutive processes. Ambient air flows through an air contactor that is packed with an aqueous solvent that dissolves CO_2 to form an inorganic solution via an exothermic reaction [11]. This inorganic CO_2-rich solution flows to the pellet reactor where it reacts with calcium hydroxide to form calcium carbonate ($CaCO_3$) and simultaneously recycle the inorganic hydroxide. The most energy-intensive process takes place in the calciner where calcination takes place by heating the solution to break the bonds between the calcium oxide (CaO) and CO_2. This endothermic reaction requires a temperature of 900 °C to free the CO_2 at ambient pressure. The CO_2 is compressed for transportation and the solid CaO is recycled in the slaker by forming a suspension with water [11]. The purity of the CO_2 ranges between 97 to 99 % [13], which is lower than for the adsorption process. The company Carbon Engineering (CE) is one of the leaders in commercialization of the absorption process [12].

The complete adsorption cycle involves at least three consecutive processes. The adsorption process differs from the absorption process in the way that a solid sorbent is used to capture CO_2. Ambient air flows through a column with an integrated filter capturing the CO_2 and releasing CO_2-dilute air back into the atmosphere. The column is vacuumized and pressurized with steam once the filter is saturated with CO_2. Desorption of CO_2 follows by applying thermal energy to the column and thereby heating the filter to a temperature of 100 °C to desorb the CO_2 [11] with a purity >99 % [13]. The column is cooled in a final step for the recycling of the filter. The company ClimeWorks (CW) is one of the leaders in commercialization of the adsorption process [12].

Economic aspects. A DAC system requires significant surface areas to meet economically feasible quantities of captured CO_2 due to these dilute atmospheric air CO_2-concentration [11]. To put in perspective, a DAC system, based on current technologies, captures 20 metric tons of CO_2 per squared meter annually compared to the six million metric ton emitted by a one gigawatt coal power plant [11]. This implies that a 300.000 squared meter capture system is required to balance

the CO_2 emitted by one coal power plant. The demand for these large capture systems drive the costs, which have been estimated to range from 90 to 550 EUR ($100 to $600) per metric ton of CO_2 captured [12] [13]. An important consideration, next to scaling and costs, is the location of the DAC system, which is decided based on further usage of the captured CO_2. The DAC system is preferred to be closely located to a storage-facility in case of temporarily or permanently storing CO_2. Contingent upon utilizing the CO_2 as a feedstock for chemical processes, e.g. for the production of synthetic hydrocarbon fuels, the preferred location of the DAC system is to be closely located to the fuel production facility. An absorption DAC system requires, along with the chemicals and electrical and thermal energy, significant amounts of water for the extraction of CO_2 [3]. The location needs therefore to be in proximity of a water source.

2.1.2 Hydrocarbon fuel synthesis

A synthetic hydrocarbon fuel can be produced through hydrogenation reactions - with hydrogen as feedstock - and through direct utilization of solar energy by applying a potential difference to drive the reaction [3]. Although the latter process uses a more simplistic approach, current conversion rates are low. Most research is therefore devoted to the former approach as hydrogenation reactions occur on a mature industrial scale. There are various catalytic conversion processes that convert carbon-containing molecules with aqueous molecules into hydrocarbons. The stoichiometric ratio in which the feedstocks react determines what type of hydrocarbon fuel is synthesized. The water-gas-shift (WGS) and the reversed water-gas-shift (RWGS) reaction convert carbon monoxide into carbon dioxide (2.1) and vice versa, respectively. These processes produce the feedstock for the synthesis of i.e. ammonia and methanol (2.2) [3]. The Fischer-Tropsch reaction (2.3) converts carbon monoxide along with hydrogen into liquid hydrocarbon fuels and is widely applied for long-chain hydrocarbon fuels [3]. The Sabatier process (2.4) involves the reaction of CO_2 and H_2 into methane.

$$CO + H_2O \rightarrow CO_2 \ + H_2 \tag{2.1}$$

$$CO + 2H_2 \ \rightarrow CH_3OH \tag{2.2}$$

$$(2n+1)H_2 \ + nCO \rightarrow C_nH_{2n+2} + nH_2O \tag{2.3}$$

$$CO_2 + 4H_2 \rightarrow CH_4 + 2H_2O \tag{2.4}$$

Methane uses a direct route for hydrogenation to a synthetic hydrocarbon fuel utilizing CO_2 as carbon-containing molecule. The production of synthetic natural gas (SNG) is an exothermic reaction and the reaction occurs at temperatures of 400 °C and a pressure of 20 bar [4]. This mature technology producing SNG is being employed on increasing industrial scale [4] [15] [16]. There are commercial methanation plants that can produce SNG in a price ranging from 0.07 to 0.90 EUR/kWh SNG [4] [16], compared to an average European natural gas price of 0.067 EUR/kWh in 2019 [17].

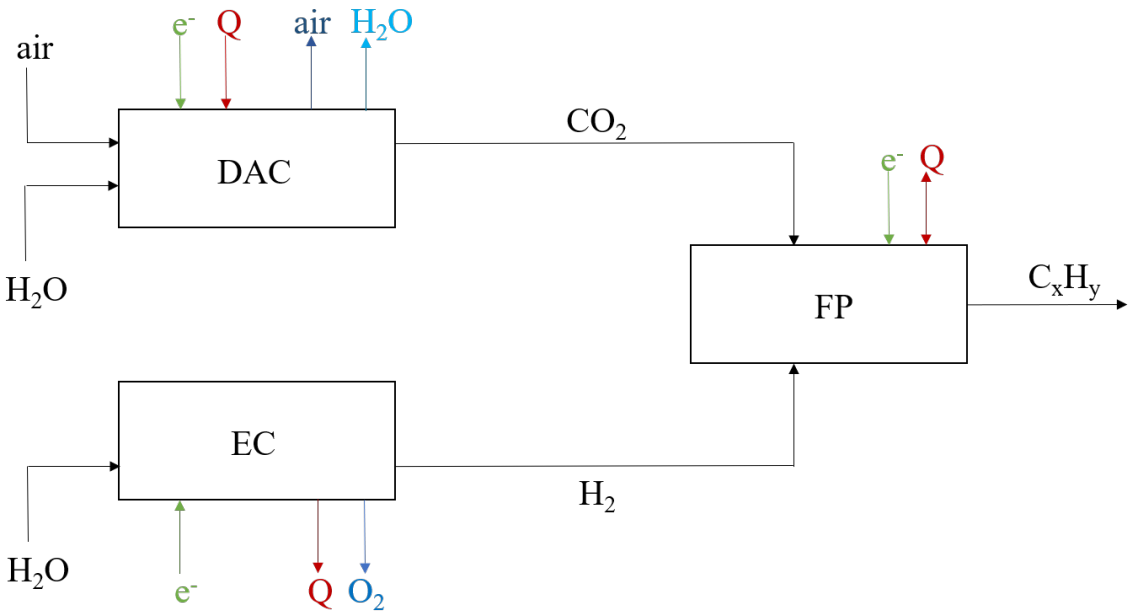

Figure 2.2: Mass and energy flows to the DAC and electrolyzer cell (EC) for the synthesis of the hydrocarbon fuel in a fuel production (FP) facility.

The conversion of the CO_2 captured in a DAC-unit along with H_2 produced in an electrolyzer unit into a synthetic hydrocarbon fuel can potentially produce CO_2-neutral hydrocarbon fuels (Figure 2.2). CO_2 neutrality requires an overall net CO_2 emission of zero, meaning that the electrical and thermal energy used in both the DAC-unit and electrolyzer system are generated CO_2-free. Additionally, the electrical energy for the compression of both feedstocks and the thermal energy to drive the chemical reactions need to come from RES.

Chapter 3

Methodological Framework

Insight in the realization and optimization of the design of a synthetic hydrocarbon fuel production system will be gained by extending on previous work [5] [8] that focused on designing a decentralized MES and modeling the framework along with technology assessments. The MES is defined in the self-built [8] energy HUB (eHUB) tool written in Matlab using mixed-integer linear programming (MILP) and represents different energy carriers and conversion and storage techniques. The MILP includes binary variables that represent the performance of the energy conversion technologies and the total cost of the selected technologies. The model returns the optimal design in terms of technology selection and size and optimal operation profile based on given weather conditions, electricity and gas prices, CO_2-emissions, and energy demand profiles. All input is implemented in an hourly interval and returns the energy demand ditto.

3.1 Problem formulation

The objective function of the optimization problem aims at minimizing the total annual cost J by allocating the required technologies while minimizing any violation. The total annual cost J comprise the sum of the total annualized capital cost J_c, operation cost J_o, maintenance cost J_m, and cost of emitting CO_2 J_{CO_2}, respectively

$$J_c = \sum_{i \in M} (\lambda_i S_i + \mu_i)\omega_i \tag{3.1}$$

$$J_o = \sum_{j \in N} \sum_{i \in M} \sum_{t=1}^{T} (u_{j,t} U_{j,i,t} - \nu_{j,i,t} V_{j,i,t}) \Delta t \tag{3.2}$$

$$J_m = \sum_{i \in M} \psi_i J_{c,i} \tag{3.3}$$

$$J_{CO_2} = \sum_{j \in N} \Big(\epsilon_j \Big(\sum_{i \in M} \sum_{t=1}^{T} U_{j,i,t} \Delta t \Big) \cdot p_{CO_2} \Big) \tag{3.4}$$

where λ_i and μ_i represent the variable and fixed cost coefficients for the i-th technology of the set M. S_i represents the unit size and ω_i is the annuity factor included to compute the equivalent annual capital cost and based on an interest rate of 6%. The annual operation cost is calculated based on the electricity import and export prices, u and v, and powers, U and V, respectively, depending on the energy carrier j, technology i, and time instant t. The annual maintenance cost set as a fraction ψ of the annual capital cost for the i-th technology. The cost of CO_2 emitted or gain from CO_2 captured is based on the specific CO_2 emission factor per carrier j and the cost of CO_2 p_{CO_2}, set to 20 EUR per metric ton CO_2 emitted [18].

The objective function with its defined input data, determined decision variables and imposed constraints is solved by branch-and-bound heuristics using Gurobi v8.02 [19]. The optimization problem is mathematically formulated as MILP and can be written as

$$\begin{aligned} \min_{x,\,y} \quad & \mathbf{c}^T \mathbf{x} + \mathbf{d}^T \mathbf{y} \\ \text{s.t.} \quad & \mathbf{A}\mathbf{x} + \mathbf{B}\mathbf{y} = \mathbf{b}, \\ & \mathbf{x} \geq \mathbf{0} \in R^{\mathbf{N}}, \mathbf{y} \in N^{\mathbf{M}} \end{aligned} \tag{3.5}$$

where $\mathbf{c}$ and $\mathbf{d}$ represent the cost vectors, $\mathbf{A}$ and $\mathbf{B}$ describe the constraints and $\mathbf{b}$ is the set constraint. These include weather profiles, hourly solar irradiance and wind speed, energy demands, electricity prices, CO_2 emission factors and cost, and the cost and performance of the technologies. The technology selection, sizing, and scheduling, the decision on energy conversion or storage and import and export are the decision variables $\mathbf{x}$ (continuous) and $\mathbf{y}$ (binary). The constraints are based on (i) the thermodynamic behavior of the selected technologies and network characteristics, (ii) the energy balances that ensure an overall balance for all energy carriers by imposing the sum of the imported and generated electrical and thermal energy to equal the exported and consumed energy,

and (iii) size of the area available for renewable energy conversion technologies. $\mathbf{N}$ and $\mathbf{M}$ indicate the dimension of the decision variables.

3.2 Input data

The input data required for solving this optimization problem consists of annual weather profiles in an hourly interval. These include global horizontal solar irradiance (GHI) and wind speeds near hub height. The energy output of the MES corresponds to the time-dependent synthetic hydrocarbon fuel demand. The day-ahead electricity prices and the price of emitting CO_2 are the input prices to the MILP. The cost per metric ton of CO_2 captured for the DAC technology and the cost per fuel output for the fuel synthesis technology are inputs as well as the thermodynamic performance of both technologies. The input data of the MILP implementation are time-dependent profiles for 2018:

i. Historic annual weather profiles in an hourly interval including global horizontal solar irradiance (GHI), $\mathbf{I} \in \mathbf{R^T}$, and wind speeds at hub height, $\mathbf{v_{wind}} \in \mathbf{R^T}$, where T indicates the length of the time horizon, being $T = 8760$.

ii. Historic day-ahead electricity prices for import and export of electricity, $\mathbf{u_e} \in \mathbf{R^T}$. The import and export price is considered equal and fluctuates in an hourly-resolution due to the variability of the energy mix.

iii. The fuel demand is the energy output of the MES and corresponds to the time-dependent synthetic hydrocarbon fuel demand, $\mathbf{F} \in \mathbf{R^T}$.

iv. The price of emitting CO_2, $\mathbf{u_{CO_2}} \in \mathbf{R^T}$, is included as an hourly static input.

v. The set of available technologies including their thermodynamic behavior and costs.

3.3 Methods

Two consecutive methods are applied for analyzing the optimal design of a MES aimed at matching a synthetic hydrocarbon fuel demand. The first method is investigating the behavior of the technologies selected by the eHUB tool when applying a static electrical and thermal energy and hydrogen demand (Figure 3.1). The DAC and fuel production (FP) technology are left outside the boundary of the eHUB tool and are represented as a static black box with solely an energy demand. The second method is investigating the behavior of the technologies selected by the eHUB tool of the optimal

design when implementing the dynamic behavior of the DAC and FP technology (Figure 3.2). Both a static and a dynamic synthetic fuel demand are simulated.

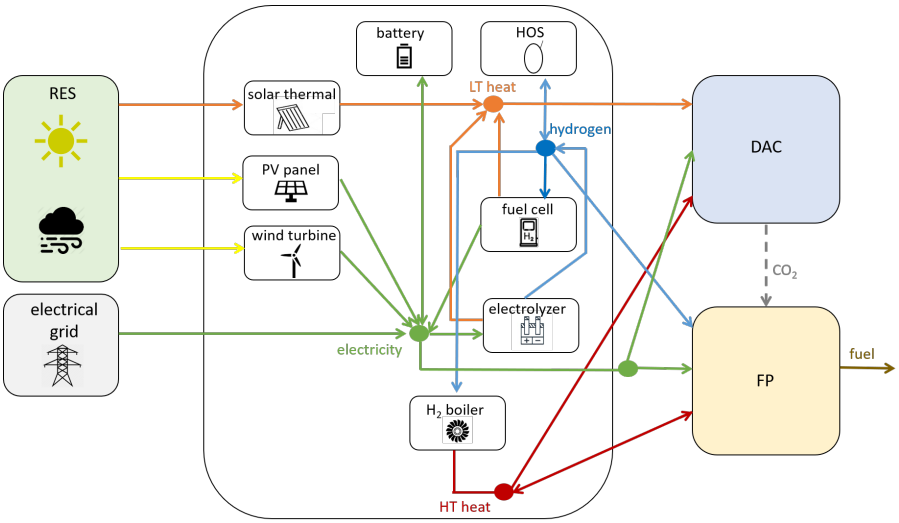

Figure 3.1: The DAC and FP system simulated as a black box with a static energy demand and CO_2 and SNG output, respectively.

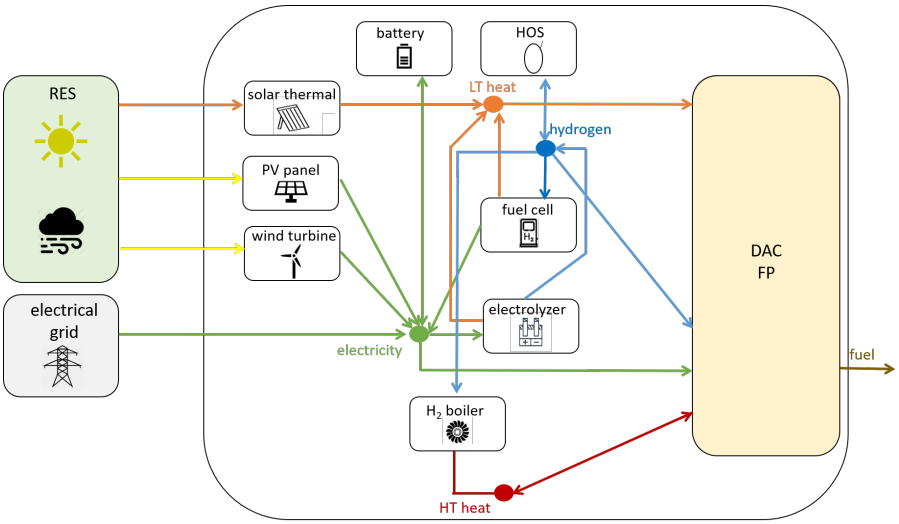

Figure 3.2: The DAC and FP system implemented in the tool as a technology with dynamic behavior.

Chapter 4

Case Study

The technology selection is based on the demand of SNG delivered by the MES. The production of SNG requires the conversion of energy carrier to another, which can come from either RES or the electrical grid. Energy delivered by RES needs to be converted to either electrical energy or thermal energy. Photovoltaic (PV) panels and wind turbines (WT) are selected for the conversion of solar irradiance and wind energy, respectively, to electrical energy. Solar thermal (ST) collectors are selected for the conversion of solar thermal irradiance to low temperature (LT) heat (up to 100 °C) [20]. The MES can be connected to the electrical grid to allow for electricity import. A hydrogen-boiler is selected as a carbon-neutral technology for the conversion to high temperature (HT) heat ($>$ 1000 °C) [21]. The electrolyzer cell (PEMEC) and fuel cell (PEMFC) are two power-to-gas (PtG) technologies that are selected for hydrogen production and electricity generation, respectively. The PEMEC is chosen based on its promising properties over its predecessor Alkaline Electrolyzer Cell (ALKEC) [3]. Both the PEMEC and PEMFC release LT heat during operation. A lithium-ion (Li-ion) battery and hydrogen storage tank (HOS) are selected to cope with the intermittent behavior of the RES.

The technology selection differs between the (HT) absorption and (LT) adsorption process. The temperature of the heat for the absorption process is higher due to the heat demand of 900 °C to drive the calcination process. The temperature output of the ST collectors, PEMEC, and PEMFC is not sufficient to reach temperature higher than 100 °C and can therefore not be selected for the absorption process. This means that the combustion of hydrogen in a hydrogen-boiler is necessary to meet the HT heat demand (Figure 4.3).

The temperature of the heat required for the desorption process in the adsorption process is 100 °C, which partially allows for the usage of LT heat technologies. The temperature of the heat released by the PEMEC and PEMFC is 70 °C, which is not sufficient for the adsorption process. The fraction of the energy content η of the heat released during operation is determined based on a constant outside temperature of 25 °C (4.1). Heat captured by ST collectors is able to meet the temperature requirements but cannot provide heat during times without solar irradiation. The combustion of hydrogen is necessary to meet the total heat demand (Figure 4.4).

$$\eta = (70 - 25)/(100 - 25) \cdot 100\% = 60\% \tag{4.1}$$

4.1 Technical characteristics DAC and FP

The annual SNG output is set based on a fixed annual carbon dioxide demand of capturing one megaton CO_2. The electrical and thermal energy and hydrogen input is set equal to producing this fixed amount of SNG. Data from three sources is compared: theoretical modelling of the adsorption process by the University of Utrecht (UU) [22], empirical data of the adsorption process by Clime-Works (CW) [13] and theoretically determined data based on the absorption process by Carbon Engineering (CE) [14] (Figure 4.1).

The DAC and FP are modelled as a coupled technology to avoid having to implement a mass balance for the CO_2 flow. The dynamic behavior, start-up/shut-down and ramp-up/down time, of the DAC-FP technology is simulated to equal the dynamics of the adsorption process and, hence, set at three hours and one hour, respectively. The adsorption process is believed to be the bottleneck of the DAC-FP technology as the start-up for methanation usually happens within an hour [15].

Table 4.1: Energy demand of the DAC processes.

Data source	Thermal energy [MJ/kg CO_2]	Electrical energy [MJ/kg CO_2]
adsorption - UU	29.7	2.12
adsorption - CW	7.20	1.62
absorption - network	4.92	1.44
absorption - autarky	4.92	0.91

4.1.1 DAC system

The electrical and thermal energy demand of both DAC capturing processes are obtained through empirical-derived data from Carbon Engineering (absorption) and Climeworks (adsorption) provided in energy content per metric ton captured CO_2 (Table 4.1).

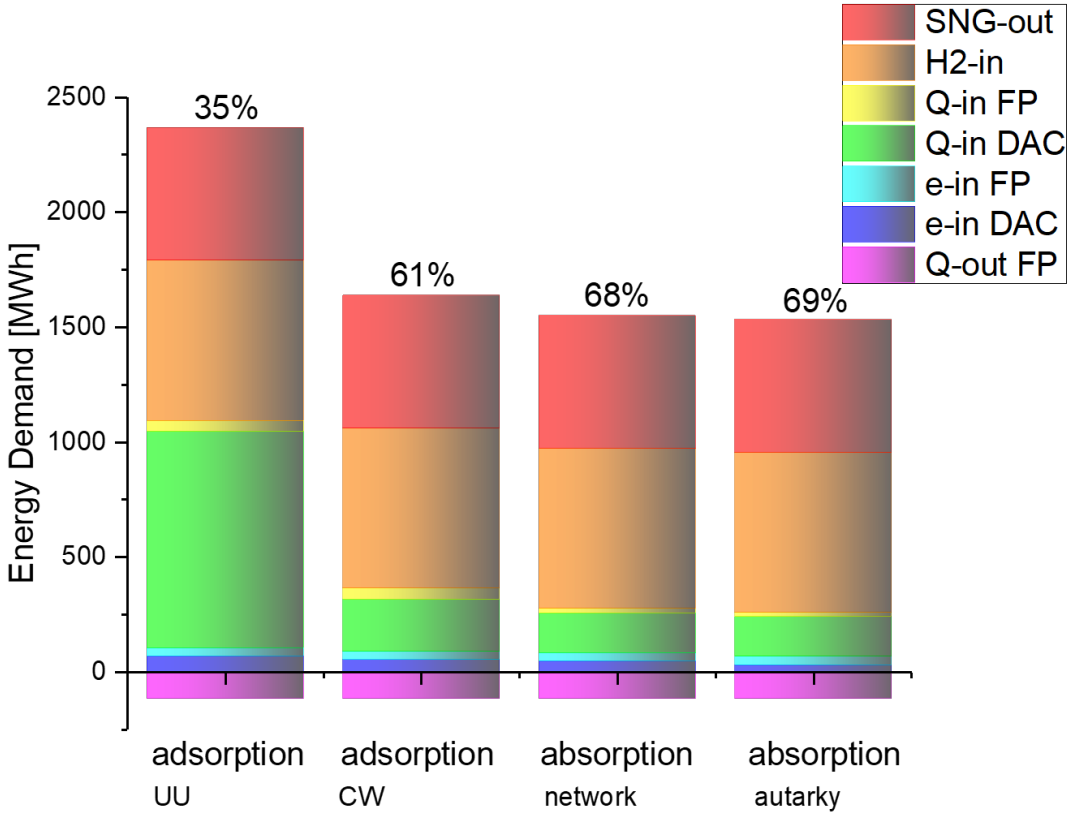

Figure 4.1: Energy demand and output of the DAC and FP for the four studies provided with each process' efficiency.

4.1.2 FP system

The H_2 demand fed into the FP is based on the molar stoichiometric ratio described in Chapter 3. Methanation takes place at a temperature of 400 °C and needs electrical energy for the compression of CO_2 from ambient pressure to 20 bar [4] [15]. The compression of H_2 to 20 bar takes place in the

PEMEC and is transported under pressure from the PEMEC to the FP. The ideal work required for compression $W_{\text{compression}}$ is approached using

$$W_{compression} = n_{CO_2} \cdot \Delta P \tag{4.2}$$

where n_{CO_2} is the flow rate of CO_2 and ΔP the change in pressure. The net thermal energy demand of the FP depends on the heat necessary to start the Sabatier process and the exothermic behavior of this process. The energy required to heat or cool the CO_2 from 100 °C or 900 °C Q_{in} (the temperature of the CO_2 from the absorption and adsorption processes, respectively) to 400 °C, is estimated using

$$Q_{in,i,j} = n_{i,j} \cdot c_p^{i,j} \cdot \Delta T_{i,j} \tag{4.3}$$

where c_{p} represents the specific heat of CO_2 or H_2, ΔT is the change in temperature, and n_{H_2} being the flow rate of CO_2 and of H_2, respectively, for $i = CO_2$ and $j = H_2$. The temperature-dependent specific heat of CO_2 and H_2 is averaged and assumed to be linear. The temperature of the H_2 - either from the HOS or directly obtained from the electrolyzer unit - is assumed to be 25 °C. The heat released by the exothermic methanation reaction Q_{out} is approached using

$$Q_{out} = \Delta H \cdot \dot{n}_{SNG} \tag{4.4}$$

being based on the change in enthalphy ΔH and the molar flow rate of the SNG $\dot{n}_{\text{SNG}}$. The temperature of the heat required to start the methanation process is higher than the LT adsorption process of the DAC but is not considered in the interest of computation time, supported by the low total thermal energy demand and the exothermic behavior of the FP system.

4.2 Economic characteristics DAC and FP

The capital expenditure (CAPEX) of the DAC is broken down into the material price of the column and the packing of the absorption process as these are believed to contribute most to the total cost [23]. These costs are tripled to estimate the total investment of the DAC by taking into account auxiliary costs and sum up to 234 EUR per metric ton CO_2 captured, which is in line with literature presenting cost ranging from 90 to 550 EUR per metric ton CO_2 captured [12] [13]. The CAPEX of the FP plant is expected to be 324 EUR per kilowatt SNG based on existing methanation plant

costs ranging from 208 to 440 EUR per kilowatt SNG [24]. The CAPEX of the DAC and FP add up to a total CAPEX of 730 EUR per kilowatt SNG. The lifetime of the DAC-FP technology is expected to be 25 years and operational expenditures (OPEX) are set up to 5 % of the investment costs [24]. The CAPEX and OPEX costs are based on present-day parameters and might half in the coming decades [13].

4.3 Case Study

The two methods described in Chapter 3 will be applied on four geographic locations and two operation modes. The influence of these parameters on the optimal design is essential in understanding the behavior of the MES for the production of SNG.

4.3.1 Geographic locations

Four geographic locations are selected to analyze and compare location-specific results based on the difference in solar irradiation, wind speeds, and electricity prices (Figure 4.2). The Netherlands is chosen as base case, Spain is chosen for its large annual solar irradiation in combination with the European electricity market, and the United Arab Emirates (UAE) and California are chosen based on their large annual and relatively constant solar irradiation.

Table 4.2: The source of the geographic dependent input data.

Geographic location	Solar irradiation [W/m^2]	Wind speed [m/s]
Utrecht, the Netherlands	Solcast [h]	KNMI [h]
Malaga, Spain	Solcast [h]	EnergyPlus [avg month]
Abu Dhabi, UAE	Solcast [h]	EnergyPlus [avg month]
California, USA	Solcast [h]	EnergyPlus [avg month]

Data collection of representative electricity prices outside Europe is proven difficult, which why is chosen to the implementation of monthly-averaged electricity prices. Wind speed data collection outside the Netherlands is also based on monthly-averaged data. Hourly resolution solar global irradiation data of 2018 for the geographic locations is obtained from Solcast [25] and wind speed profiles of 2018 is obtained from KNMI [26] (hourly) for the Netherlands and EnergyPlus [27] (averaged over a month) for Spain, United Arab Emirates (UAE) and United States of America

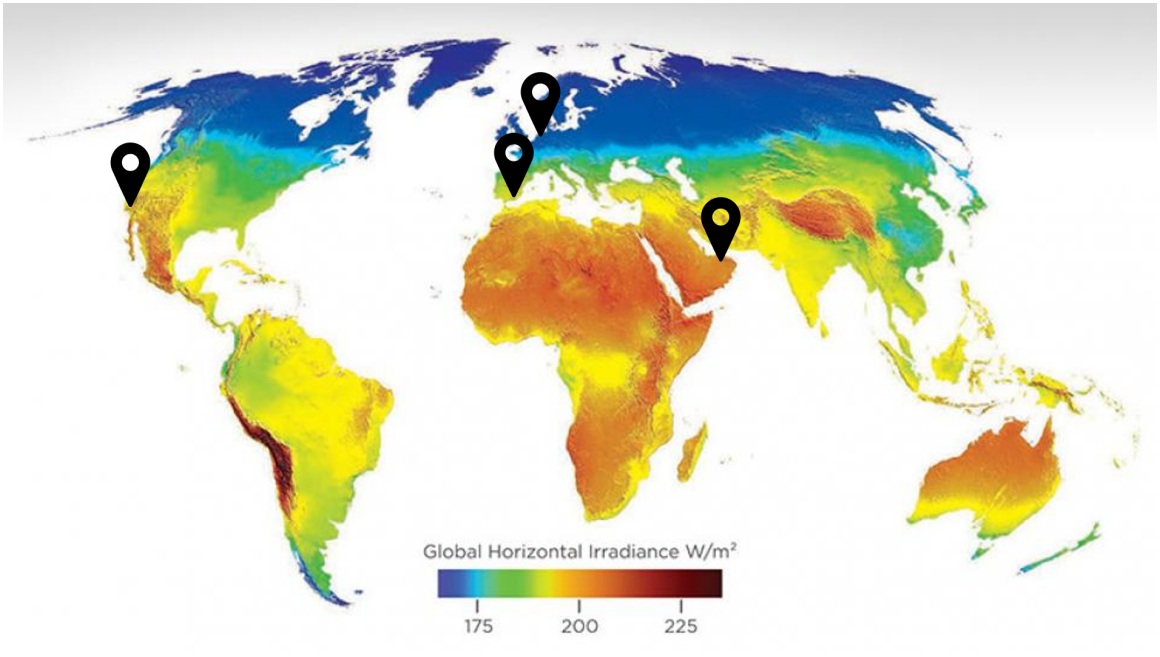

Figure 4.2: Geographic specific global horizontal solar irradiation [1].

(USA) (Table 4.2). Geographic specific hourly resolution electricity prices (day-ahead) of 2018 for Europe are available through entso-e [28]. The available data for the electricity prices of the UEA and USA is averaged over the month and is therefore translated to an hourly interval based on these monthly fluctuations [29].

4.3.2 Operation Modes

Two operation modes are considered: one when allowing for electricity import from the electrical grid (network) and the other when forcing a high penalty on electricity import and thus implementing a fully self-sufficient MES (autarkic system). The distinction between the two operation modes will provide insight in the economic feasibility of a fully autarkic system. There are no area constraints imposed on the available land of the renewable energy conversion technologies as well as there are no constraints imposed on the capacity of the allowed electricity import.

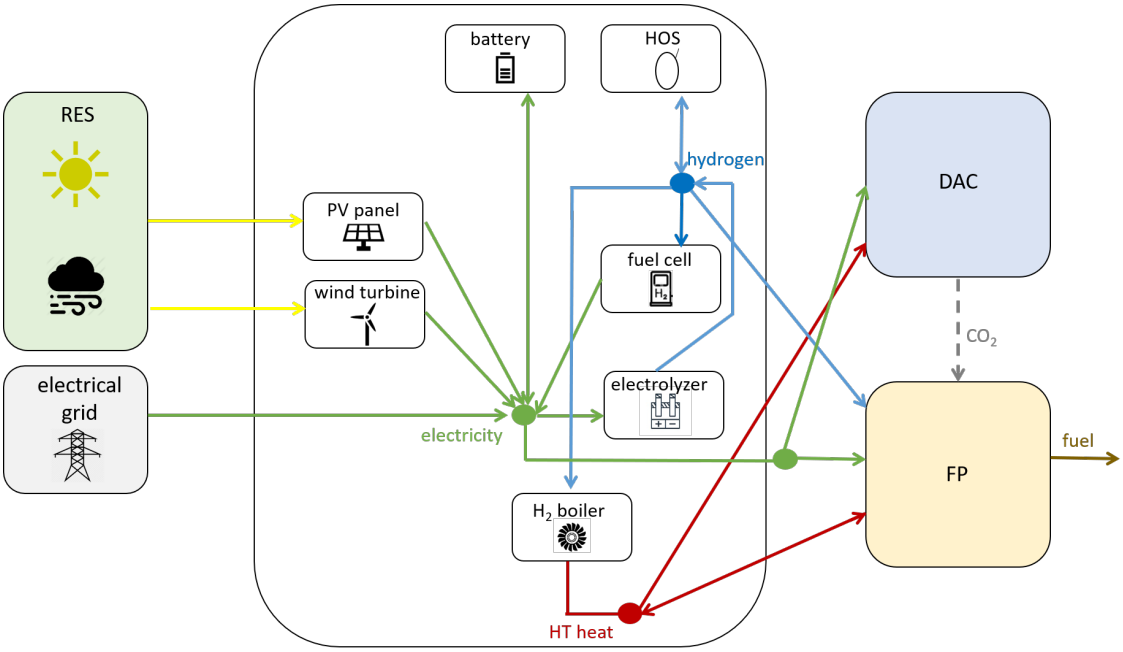

Figure 4.3: Technology selection for the (HT) absorption process.

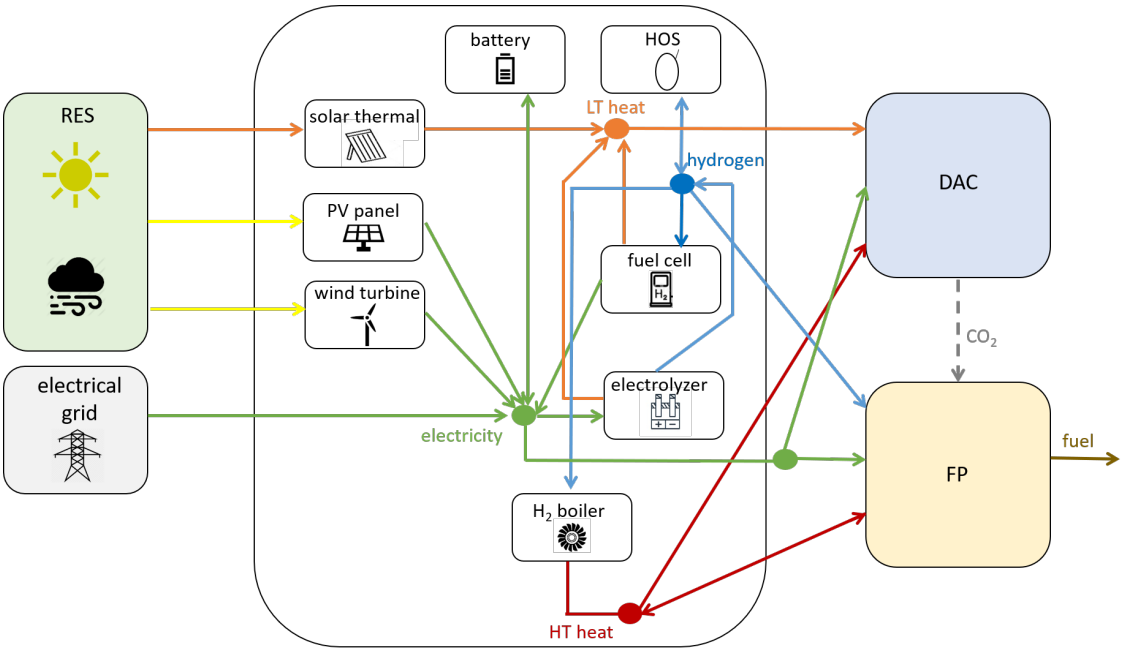

Figure 4.4: Technology selection for the (LT) adsorption process.

Chapter 5

Results

The behavior of the technologies interacting within the MES for the production of SNG is observed and described for six different systems in four geographic locations (Table 5.1). The results obtained from applying a static energy demand are interpret and displayed followed by an explanation of the dynamic behavior of the combined DAC-FP technology including a dynamic SNG demand.

Table 5.1: The six considered and compared systems.

Name	Capture technique	Operation mode
network UU	adsorption	allowed import
network CW	adsorption	allowed import
network CE	absorption	allowed import
autarky UU	adsorption	no allowed import
autarky CW	adsorption	no allowed import
autarky CE	absorption	no allowed import

5.1 Method I - static demand

The technology selection depends on the CO_2-capture process, operation mode, and geographic location. The geographic location of the Netherlands is used as example to explain the changes in optimal design due to these specifications. The thermodynamic characteristics of the other geographic locations is explained and added to Appendix B.

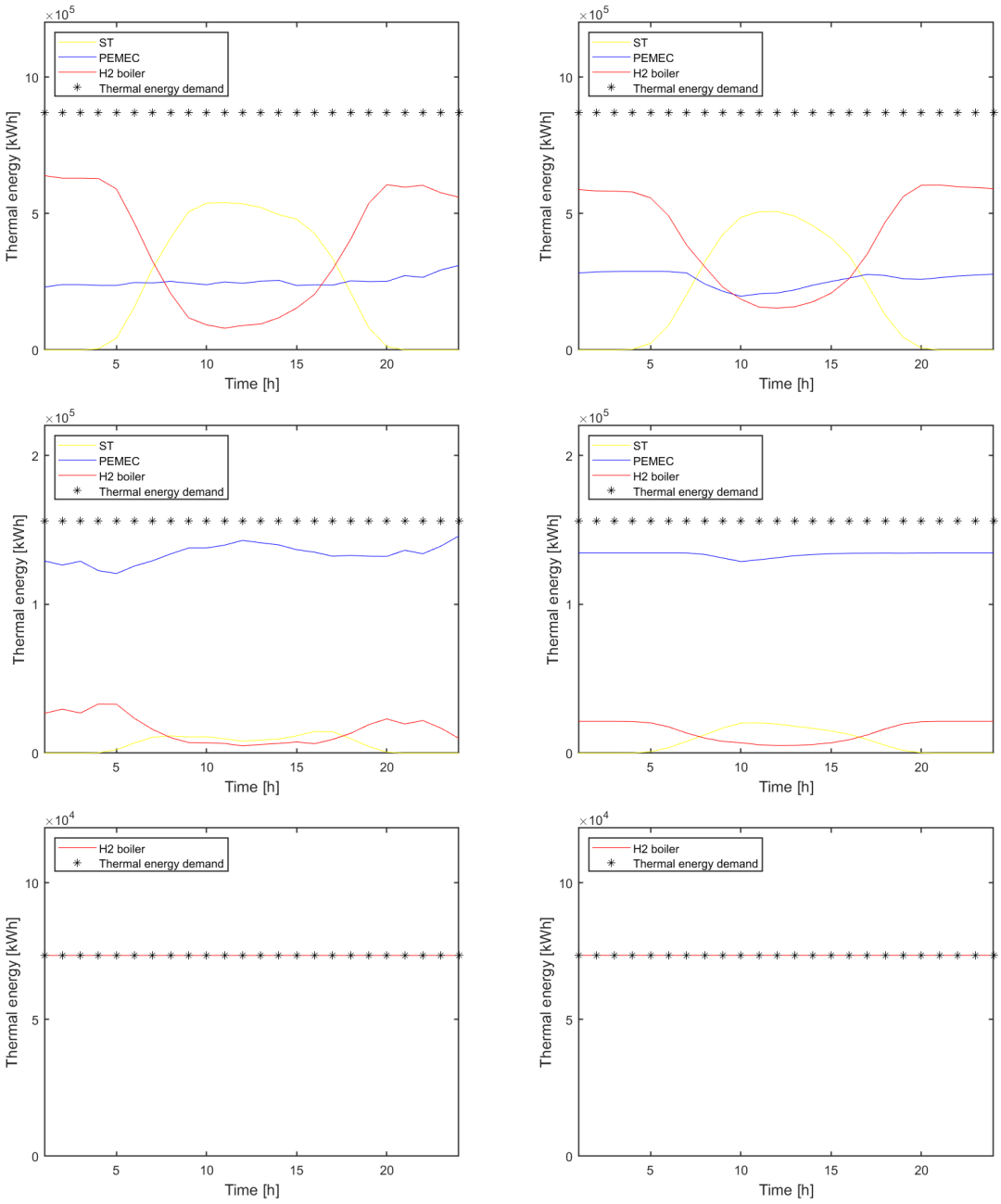

Figure 5.1: Share of thermal energy sources to match thermal energy demand of DAC-FP averaged over the year. Top: autarky UU adsorption (left) and network UU adsorption (right). Middle: autarky CW adsorption (left) and network CW adsorption (right). Bottom: autarky CE absorption (left) and network CE absorption (right).

Dutch system. The thermal energy demand of the UU adsorption process is over four times higher than that of the CW adsorption process. As as consequence of this significant thermal energy demand all three thermal energy technologies are roughly equally contributing to the total thermal energy demand (Figure 5.1). Most of the thermal energy demand of the CW adsorption process can be provided by the PEMEC but has to be supported by both the hydrogen-boiler and the ST collectors. The higher thermal energy output of the PEMEC for the UU adsorption process can be related to the higher hydrogen demand for the hydrogen-boiler. The thermal energy demand of the CE absorption process is supplied by solely the hydrogen boiler as only the boiler is capable of supplying heat of sufficient temperatures.

The electrical energy throughout the MES is distributed among the DAC-FP and PEMEC of which the latter has a significantly higher demand than the DAC-FP (Figure 5.2). The optimal design includes the utilization of offshore wind in all systems and is thus competing with electricity import. An increase in average electrical energy output from offshore wind is observed at the end of the day, reducing the electricity import. Electrical energy from photovoltaics is utilized for the autarkic systems only. The fluctuating electrical energy demand of the PEMEC for the UU adsorption process is caused by the appearance of relatively high solar thermal energy load during the day.

Hydrogen storage is necessary in all systems except for the CE absorption process (network configuration) as for the latter the total thermal energy demand is obtained from the hydrogen-boiler (Figure 5.3). A larger solar thermal energy output results in a larger hydrogen storage capacity. For the adsorption process the hydrogen-boiler and the PEMEC interact with ST collectors, which do not have steady thermal energy outputs. As a result of this intermittent behavior the electrolyzer needs to overproduce hydrogen which is used in times of low to no solar thermal energy output. Electrical energy storage in form of batteries is required in all autarkic systems but significantly so in the CW adsorption process. This fluctuating charge and discharge profile can be explained by the presence of a relatively smaller PEMEC than the UU adsorption process while the hydrogen storage is similar and the photovoltaic and wind energy is per electrical and thermal energy demand significantly higher. Seasonal effects on electrical and hydrogen storage capacities are observed with intensified fluctuations in summer periods due to the increase in renewable energy penetration (Appendix C).

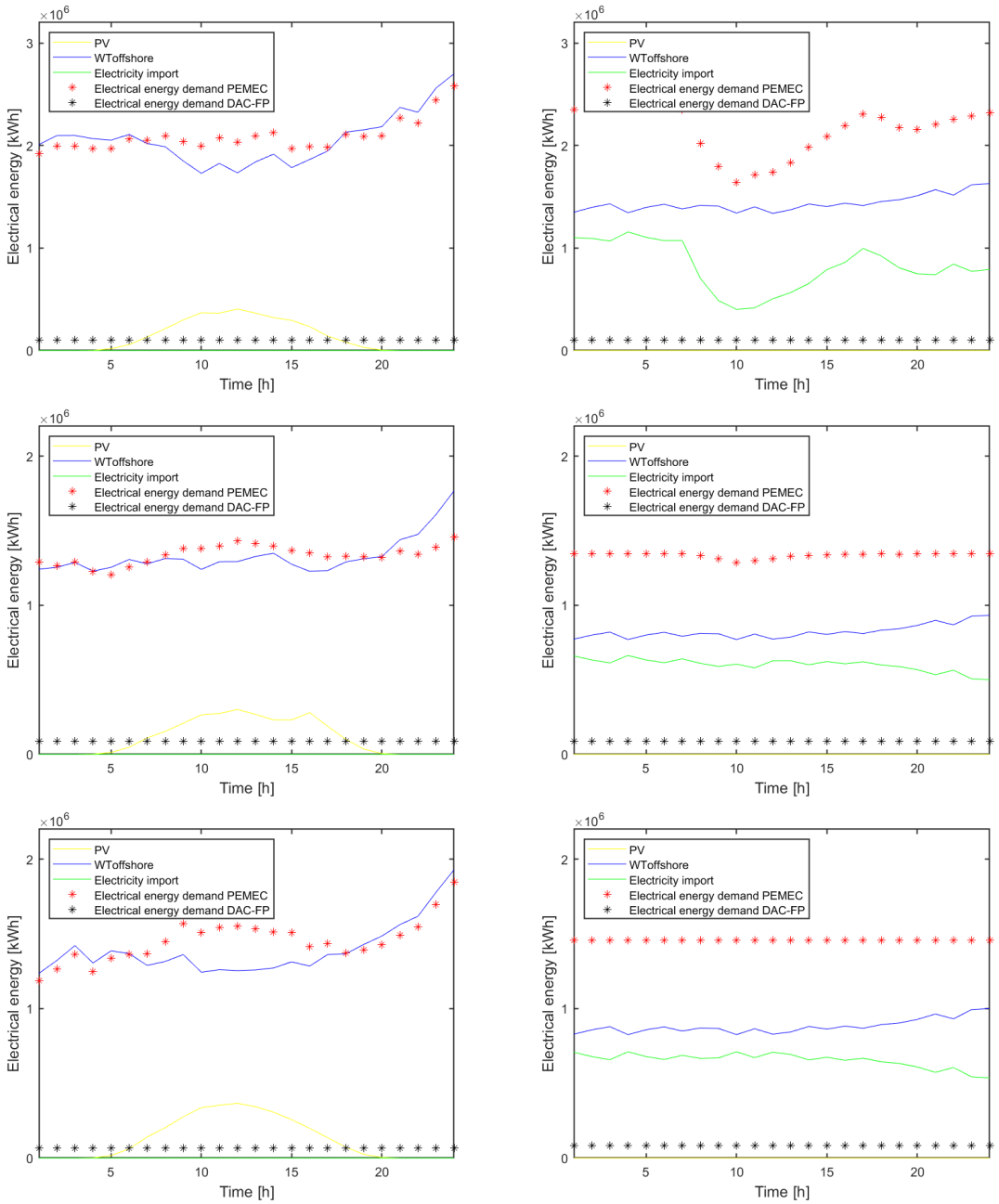

Figure 5.2: Share of electrical energy sources to match electrical energy demand of DAC-FP and PEMEC averaged over the year. Top: autarky UU adsorption (left) and network UU adsorption (right). Middle: autarky CW adsorption (left) and network CW adsorption (right). Bottom: autarky CE absorption (left) and network CE absorption (right).

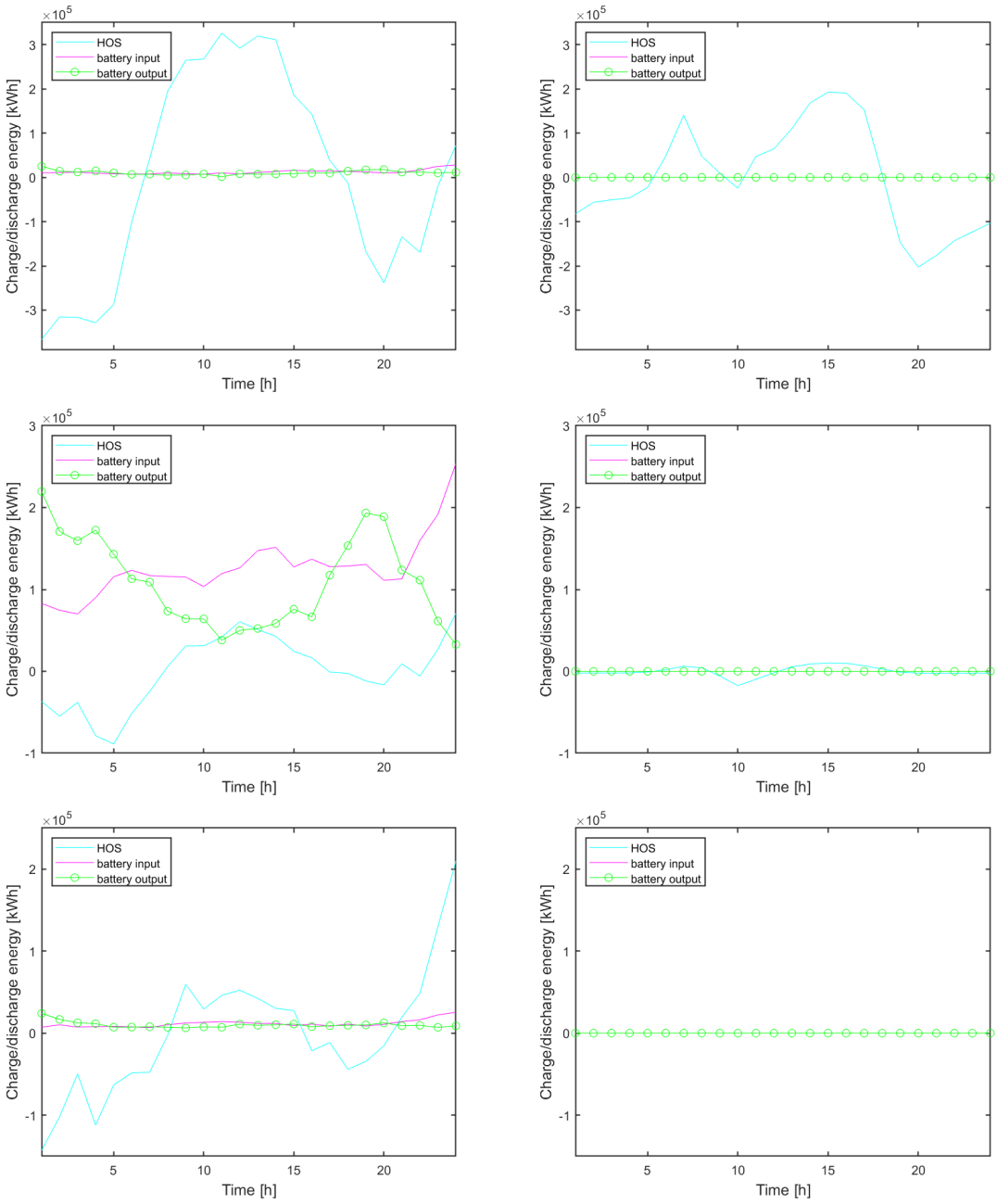

Figure 5.3: Share of electrical energy storage and hydrogen storage implemented to cope with intermittent behavior of RES. Top: autarky UU adsorption (left) and network UU adsorption (right). Middle: autarky CW adsorption (left) and network CW adsorption (right). Bottom: autarky CE absorption (left) and network CE absorption (right).

Geographic location dependence. Employing the network operation mode and allowing for electricity import leads to an optimal design of low to no RES exploitation (Figure 5.4). The optimal design for the Dutch geographic location includes the utilization of offshore wind in all systems and is thus competing with electricity import. Offshore wind energy is not considered for the other geographic locations due to the absence of offshore wind energy potential [1]. Significant area sizes are required for the realization of a fully autarkic system in all geographic locations with the UAE as outlier, exploiting up to one percent of its total area, which comes down to the same percentage when fulfilling the Dutch autarkic demand. A distinct difference in geographic location with respect to large solar irradiance (Spain/USA/UAE) and high average wind speeds (Netherlands/UAE) is observed.

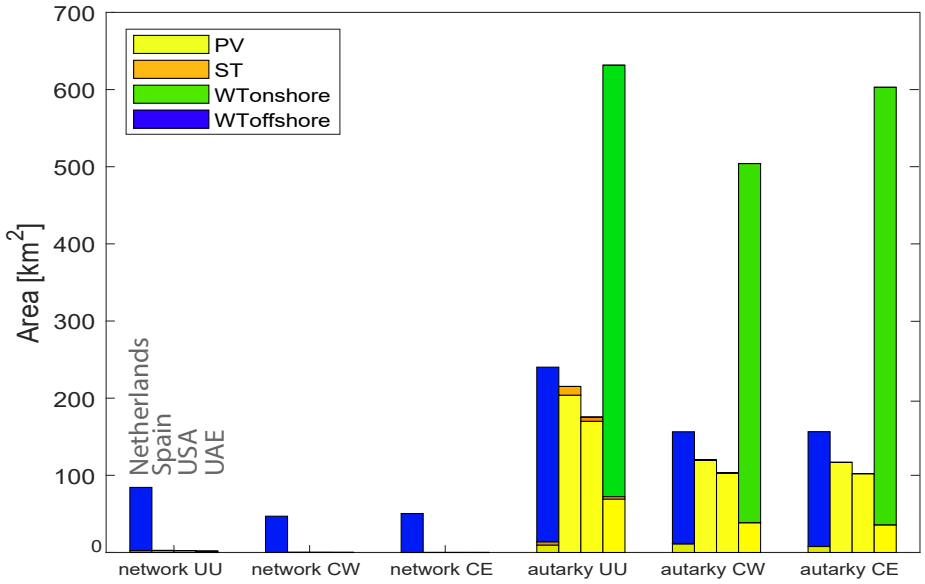

Figure 5.4: The optimal design of the total area needed to fulfill the energy demand by employing renewable energy technologies - photovoltaics (PV), solar thermal collectors (ST), and on- and offshore wind turbines (WT) - for both the adsorption process (UU and CW) and the absorption process (CE) when allowing for electricity import (network) and when being fully autarkic (autarky) for the four geographic locations.

5.2 Method II - dynamic technology

Cost of system and net emissions. The share of as well as the total annualized cost differ between the autarkic and network operation mode. The PEMEC is by far the largest contributor to the cost (over 50 % for all systems) when allowing for electricity import. The employment of RES adds significantly to the total annualized cost of the autarkic system, contributing to a share over 50 % for both adsorption and absorption processes. The countries without offshore wind exploitation (Spain, USA, and UAE) require larger electrical energy storage technologies than the Netherlands, adding up to roughly 25 % cost share. The hydrogen storage vessel, hydrogen boiler, and DAC-FP are not determininative factors to the optimization problem. The breakdown of the cost of the UU adsorption process for the Netherlands is depicted in Figure 5.5. For the cost breakdown of the UU adsorption process for Spain, USA, and UAE, see Appendix A.

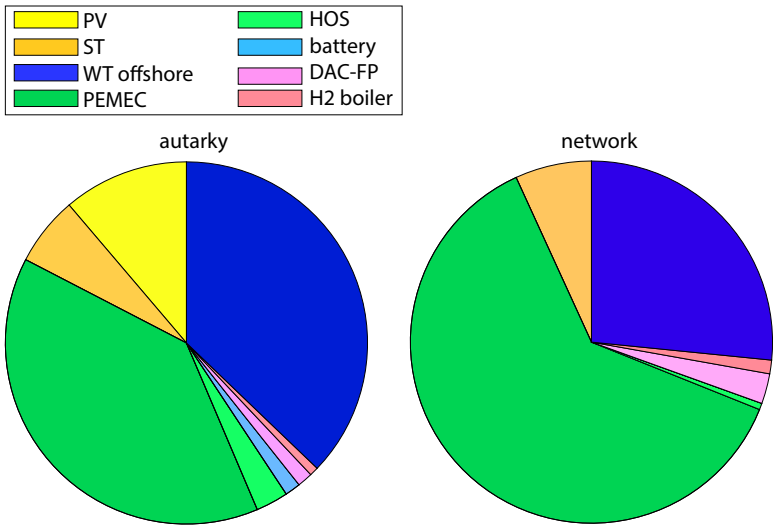

Figure 5.5: Breakdown of the annualized costs associated to the autarkic (left) and network (right) system for the Dutch UU adsorption process.

The cost of the optimal design of the absorption and adsorption process differs considerably between the two operation modes and geographic locations (Figure 5.6). The cost of producing SNG varies from 0.14 to 2.30 EUR per kWh SNG (LHV), which is in line with literature [4] [24]. No significant difference is observed between the CW adsorption and CE absorption process. The UU adsorption process, on the other hand, is less cost-effective due to its large thermal energy demand. Electricity

import from the grid is in most systems significantly cheaper than exploiting RES and being fully autarkic. The implementation of offshore wind turbines, however, reduces the cost of the autarkic system with at least a factor two. The highest cost is observed for the Spanish UU autarkic system, caused largely by its large electricity storage demand.

All network-connected systems carry a positive carbon-footprint, except for the Dutch. The implementation of offshore wind turbines results in net negative CO_2 emissions; CO_2 emitted during SNG combustion not considered, even when allowing for electricity import. This compared to annual CO_2 emissions ranging from 700,000 to 1,700,000 metric ton annually for network systems without implementation of wind turbines. A fully autarkic system sums up to the predetermined value of one megaton emissions avoided.

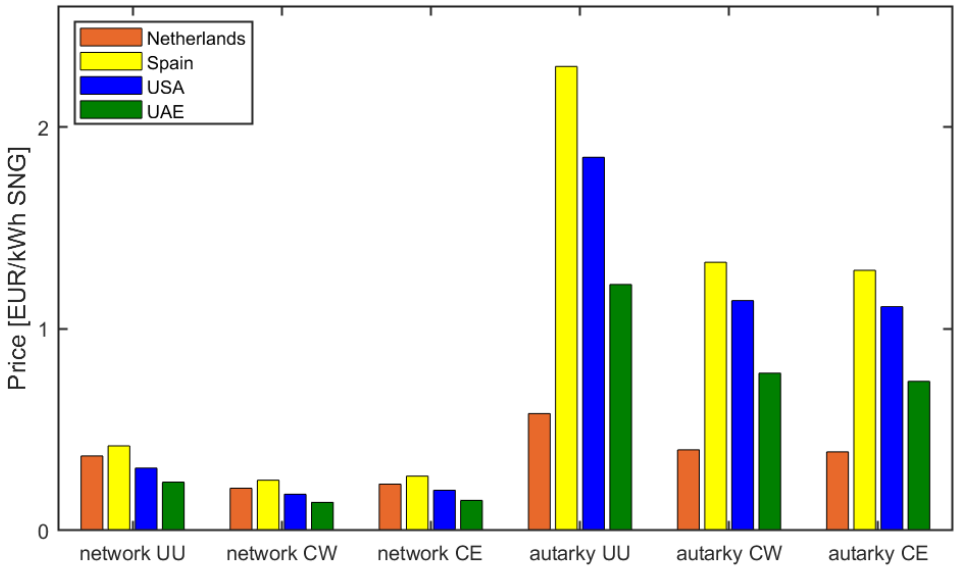

Figure 5.6: The price of the MES per kWh SNG for the adsorption and absorption process for both operation modes and all geographic locations.

Sensitivity analysis. The investment cost of the technologies is a function of time leading to uncertainties in future predictions. Investigating the change in optimal design as result of lower electricity prices, declining cost for renewable energy technologies, and higher CO_2-taxes, might reduce the uncertainty and shows the change in optimal design.

The electricity price is an important player in the total cost per kWh produced SNG. Currently, lowest electricity prices are present in UAE being the reason for the lowest total price per kWh produced SNG (Figure 5.6). Reduction of electricity prices shift the optimal design to a less autarkic system. These prices are associated to the energy mix and, thus, linked to RES exploitation. This effect is, however, not considered here. Introducing an electricity price half and one tenth of the current electricity price affects the optimal design of all network systems in the way that renewable energy technologies are less to not being employed. The percentile change in price allows for comparison between the systems and shows price reduction from 35 % for countries with high RES exploitation (NL) to 50 % for countries with low RES exploitation and high electricity prices (SP) (Figure 5.7). Reduction of the electricity price has the largest impact on the Dutch optimal design where the system stalls employment of RES from an electricity price lower than 70 %.

A tripling of the CO_2-price to 60 EUR per metric ton CO_2, which is believed to be the price CO_2 needs to have to meet the Dutch Climate Agreements, seems to have limited impact on the optimal design. The exploitation of offshore wind turbines in Dutch systems decreases the price of SNG as its carbon footprint is negative for all systems, except UU adsorption network system. In all geographic locations and network systems, a tripled CO_2-price increases the price of SNG but does not influence their optimal designs in terms of technology selection and does not yet results in higher penetration of renewable energy technologies.

The price of renewable energy technologies, particularly of PV, has dived over the last decades and as PV plays a role in the optimal design of all geographic locations, future price drops of PV will influence results. Halving the investment cost of PV, which is proven feasible within years [30], increases the total installed capacity while (i) reducing the employment of solar thermal and (ii) increasing the size of PEMEC in order to save on electrical energy storage capacity.

Dynamic demand. The introduction of a dynamic SNG demand shows the anticipated trend of necessitating larger energy storage capacities. This, along with the need for larger electrolyzer systems, renewable energy technologies, and DAC-FP, increases the cost per kWh SNG produced.

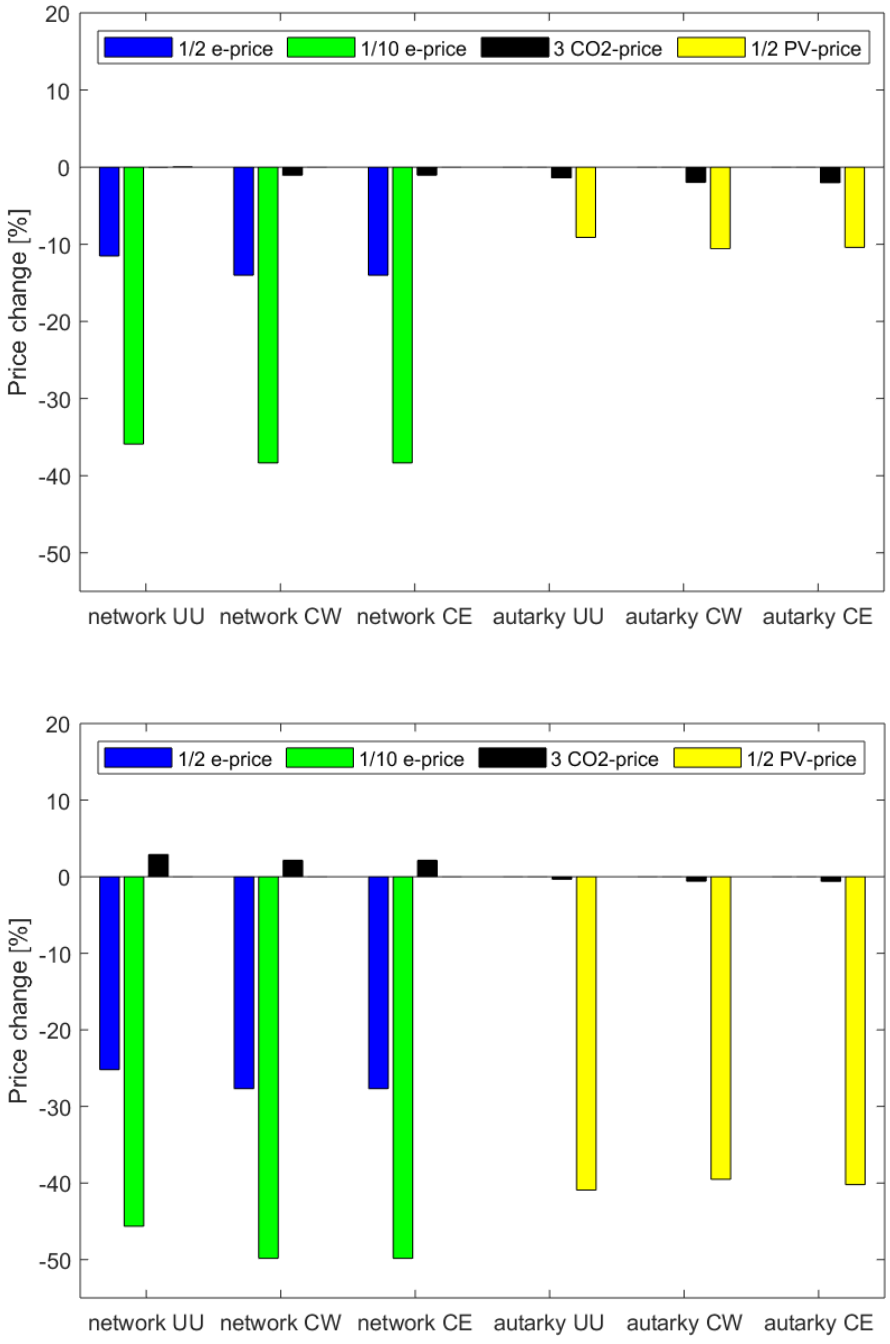

Figure 5.7: Percentile change in price for the Dutch (top) and Spanish (bottom) systems upon implementing reduced electricity prices, increased CO_2-price, and reduced PV investment cost.

Chapter 6

Discussion

The optimal designs presented in Chapter 5 are build upon consciously chosen assumptions but are subject to change. No distinction is made between the investment cost of the adsorption and absorption process. The variation in cost between those two processes is nil compared to the total cost of the system and is, thus, likely to not influence the optimal design. While operation costs are specified per geographic location, location-specific investment and maintenance cost are not considered and likely to influence the optimal design. The cost of acquiring appropriate areas of land is not taken into account, but is substantial.

The distribution and fraction of CO_2 in the air is subject to change over time and geographic location. The energy demands considered are based on a ratio of 400 ppm CO_2 in the atmosphere. Seasonal and geographic effects on this ratio are neglected in our simulations. Next to this, we assume a pure CO_2 stream exiting the DAC and entering the FP although the purity for both the adsorption and absorption process ranges around 98 %.

Technologies other than the considered technologies, such as hydro-power and geothermal, are not considered as for the relatively small-scale application of the MES. The Solid Oxide Electrolyzer/ Fuel Cell (SOEC/FC) shows promising characteristics on lab-scale and could potentially increase PtG efficiencies but is still too novel to consider. The LT heat from the PEMEC is not used for the absorption process as it is expected to contribute only minor to the absorption process. This LT heat could potentially be used for other processes in- or outside the considered MES.

A sensitivity analysis on the electricity price is performed but these prices are affected by RES exploitation and their share in the electricity mix. A coupled influence of weather patterns on elec-

tricity prices could more realistically reflect price fluctuation behavior. The carbon-intensity of the electricity mix is based on Dutch standards and applied to the other geographic locations. The coupling of carbon-intensity to the selection of renewable electricity technologies could be implemented. Connecting the FP to the electricity price will most likely not affect the production as the dynamics of the FP system are slow. The adsorption process of the DAC, on the other hand, might be affected by changes in price.

As mentioned in Chapter 2 the size of the DAC is significant given a recovery of 1 Mt CO_2 annually. However, the requirement of an area of 50.000 squared meter is negligible compared to the area needed for RES exploitation in fully autarkic systems.

In all simulations the ideal case is considered, implicating that losses in distribution within the MES are not included. This was preferred as to obtain the best case scenario outcome. Moreover, we did not include infrastructures except for electricity, heat, hydrogen, and gas distribution networks by assuming all technologies being located in proximity of each other.

Recommendations. The DAC and FP technology are implemented as coupled units, which inhibits modelling their technical and economic characteristic individually. The addition of a CO_2 mass balance to the tool allows for separate energy and mass flows between the DAC and FP. The introduction of a CO_2-storage technology - comparable to the already included hydrogen storage in salt caverns - might alter the optimal design as the adsorption process of the DAC is considered a fast response system in comparison with the absorption and fuel production process. This implicates a distinction between the adsorption and absorption process to be implemented as well. Decoupling of the DAC and FP and introduction of adsorption and absorption processes allows for the separation of temperature heat flows. Theretofore, heat flows should be characterized as LT and HT heat flows.

The production of SNG has been considered as this energy carrier *gas* had already been implemented to the eHUB tool and allowed for measuring the effectiveness of the model. Other synthetic fuels, such as methanol, gasoline, and kerosene, might be advanced options for the MES as of their suitable applications in the maritime and aviation transportation sector. A short preliminary investigation into methanol led to the observation that it decreases the system's efficiency though demanding less hydrogen. The lower LHV of methanol compared to SNG refutes the benefit.

Optimization of the CW adsorption process system showed for all designs, independent of location and operation mode, inexplicable results. As of the relatively small thermal energy demand compared to the UU adsorption process large quantities of heat are dissipated while selecting enor-

mous electrical energy storage capacities and increasing total system cost. This is not intuitive as excess electricity should be curtailed rather than stored in batteries. Discretization of the thermal energy demand starting from the UU system towards the CW system demand showed optimization limitations when its entire thermal energy demand is delivered by the PEMEC. Due to time limitations this optimization error is not yet resolved but this issue was diverted by forcing the selection of at least one extra thermal energy technology.

Chapter 7

Conclusion

This research aims at evaluating the optimal design, in terms of minimizing the costs, of a carbon neutral SNG production system and its operation upon varying electricity prices, CO_2 tax, weather data, and fuel production profile. The effects of the first two are investigated via sensitivity analyses, identifying thresholds for economic viability, while the weather profiles represent four different geographic locations around the world. The SNG production operation is varied to see the effects of a dynamic versus stable production. Special attention is payed to the interplay between the various technologies, especially the behavior of the storage technologies for different weather profiles and spatial constraints.

Significant differences in optimal design are observed between the two CO_2 recovery processes, four geographic locations, and two operation modes. The demand of HT heat for the absorption process excludes the selection of thermal technologies other than the hydrogen-boiler. The origin of this (additional) hydrogen demand - the PEMEC - is the largest contributor to the total cost in all network-connected systems. Although the LT thermal energy demand of the adsorption process allows for heat recovery from the PEMEC and solar thermal collectors, additional hydrogen-boiler are necessary to meet this demand. The large deviation in thermal energy demand of the adsorption process between UU and CW-based data increases the uncertainty in the optimal design for this process.

The optimization process is highly influenced by geographic location. The implementation of hourly profiles of solar irradiance and onshore wind speeds (and offshore wind speeds of the Netherlands) of the Netherlands, Spain, USA, and UAE demonstrate that only electricity generated

by offshore wind turbines compete with current electricity prices being the reason that only the Dutch systems carbon footprint is carbon-negative - excluding the CO_2 emitted when burning the fuel. Geographic locations with low electricity prices, with UAE as outlier, show the anticipated trend of less to no RES exploitation.

The trade-off between carbon neutral and cost-effective produced SNG varies between CO_2 recovery process and geographic location, but is mostly affected by the level of autarky of the MES. The optimal design of network-connected systems ranges between 0.14 and 0.25 EUR/kWh SNG compared to variations between 0.39 and 2.30 EUR/kWh SNG for full autarkic systems. The necessity to continuously fulfill a given SNG demand when relying on intermittent energy sources calls for not only significant area availability but also energy storage capacities.

Small-scale applications of both CO_2 recovery and SNG production have already proven to be technically feasible. This study shows that there are MES configurations capable of producing carbon-neutral SNG approaching current natural gas prices and can thus substitute fossil fuels in the near future.

Bibliography

[1] Vaisala. Resource maps. Available at https://www.vaisala.com/en/lp/free-wind-and-solar-resource-maps, accessed 06/08/2019.

[2] International Energy Agency. Tracking clean energy progress 2017. Available at https://www.iea.org/etp/tracking2017/, accessed 07/20/2019.

[3] J. Herron, J. Kim, A. Upadhye, G. Huber, and C. Maravelias. A general framework for the assessment of solar fuel technologies. *Energy and Environmental Science*, 8:126–157, 2015.

[4] K. Ghaib and F. Ben-Fares. Power-to-Methane: A state-of-the-art review. *Renewable and Sustainable Energy Reviews*, 81:433–446, 2018.

[5] P. Gabrielli, M. Gazzani, and M. Mazzotti. Electrochemical conversion technologies for optimal design of decentralized multi-energy systems: Modeling framework and technology assessment. *Applied Energy*, 221:557–575, 2018.

[6] M. Steinberg. Production of hydrogen and methanol from natural gas with reduced CO_2 emissions. *International Journal for Hydrogen Energy*, 23:419–425, 1998.

[7] J. Holladay, J. Hu, D. King, and Y. Wang. An overview of hydrogen production technologies. *Catalysis Today*, 139:244–260, 2009.

[8] P. Gabrielli, M. Gazzani, E. Martelli, and M. Mazzotti. Optimal design of multi-energy systems with seasonal storage. *Applied Energy*, 219:408–424, 2017.

[9] Het Energieakkoord. Energieopwek. Available at http://energieopwek.nl, accessed 03/19/2019.

[10] Gasunie/TenneT. *Infrastructure Outlook 2050: A joint study by Gasunie and TenneT on integrated energy infrastructure in the Netherlands and Germany.* 2019.

[11] APS physics. *Direct Air Capture of CO_2 with chemicals: A technology assessment for the APS panel on public affairs.* 2011.

[12] A. Sberegaeva and Y. Romitti. Direct Air Capture and mineral carbonation approaches for carbon dioxide removal and reliable sequestration. Available at https://www.nap.edu/read/25132/chapter/19, accessed 07/17/2019.

[13] M. Fasihi, O. Efimova, and C. Breyer. Techno-economic assessment of CO_2 Direct Air Capture plants. *Journal of Cleaner Production*, 224:957–980, 2019.

[14] D. Keith, G. Holmes, D. Angelo, and K. Heidel. A process for capturing CO_2 from the atmosphere. *Joule*, 2:1–22, 2018.

[15] J. Bremer, K. Ratze, and K. Sundmacher. methanation: Optimal start-up control of a fixed-bed reactor for Power-to-Gas applications. *American Institute of Chemical Engineers Journal*, 63:23–31, 2016.

[16] J. Baier, G. Schneider, and A. Heel. A cost estimation for CO_2 reduction and reuse by methanation from cement industry sources in switzerland. *Frontiers in Energy Research*, 6:1–5, 2018.

[17] Eurostat. Natural gas price statistics. Available at https://ec.europa.eu/eurostat/statistics-explained/index.php/Naturalgaspricestatistics, accessed 07/20/2019.

[18] Market Insiders. Co_2 european emission allowances. Available at https://markets.businessinsider.com/commodities/co2-european-emission-allowances, accessed 06/08/2019.

[19] Gurobi. Mixed-Integer Linear Programming (MILP). Available at http://www.gurobi.com/resources/getting-started/mip-basics, accessed 03/10/2019.

[20] A. Fernandez and J. Dieste. Low and medium temperature solar thermal collector based in innovative materials and improved heat exchange performance. *Energy Conversion and Management*, 75:118–129, 2013.

[21] V. Zabaykin. Hydrogen combustion under conditions of a high-temperature supersonic flow. *Heat and Mass Transfer and Physical Gasdynamics*, 55:567–572, 2017.

[22] F. Sabatino, A. Grimm, F. Gallucci, M. van Sint Annaland, G. Kramer, and M. Gazzani. Comparative assessment and optimization of Direct Air Capture via absorption and adsorption processes. *in preparation.*

[23] M. Bui, P. Tait, M. Lucquiaud, and N. Mac Dowell. Dynamic operation and modelling of amine-based CO_2 capture at pilot scale. *International Journal of Greenhouse Gas Control*, 79:134–153, 2018.

[24] M. Gotz, J. Lefebre, F. Mors, A. McDaniel Koch, F. Graf, S. Bajoh, R. Riemert, and T. Kolb. Renewable Power-to-Gas: A technological and economic review. *Renewable Energy*, 85:1371–1390, 2016.

[25] Solcast. Solar Radiation Data - historical and TMY. Available at https://solcast.com/-solar-radiation-data/historical-and-tmy/, accessed 07/02/2019.

[26] KNMI. Uurgegevens van het weer in Nederland. Available at https://-projects.knmi.nl/klimatologie/uurgegevens/selectie.cgi, accessed 07/02/2019.

[27] EnergyPlus. Weather data. Available at https://energyplus.net/weather, accessed 07/02/2019.

[28] entso-e. Day-ahead price. Available at https://transparency.entsoe.eu/transmission-domain/r2/dayAheadPrices/show, accessed 07/02/2019.

[29] EIA. United States energy information administration. Available at https://www.eia.gov/-to-dayinenergy/detail.php?id=32172, accessed 07/02/2019.

[30] Fraunhofer. Photovoltaics report. Available at https://www.ise.fraunhofer.de/content/dam/ise/de/documents/publications/studies/Photovoltaics-Report.pdf, accessed 07/30/2019.

Appendix A

Cost breakdown

The breakdown of the total annualized cost for the network and autarkic system of the UU adsorption process for Spain, USA, and UAE is presented (Figure A.1). The PEMEC contributes most to the total cost when allowing for electricity import and exploiting limited to no RES. This changes upon selecting a fully autarkic system with full penetration of renewable energy technologies.

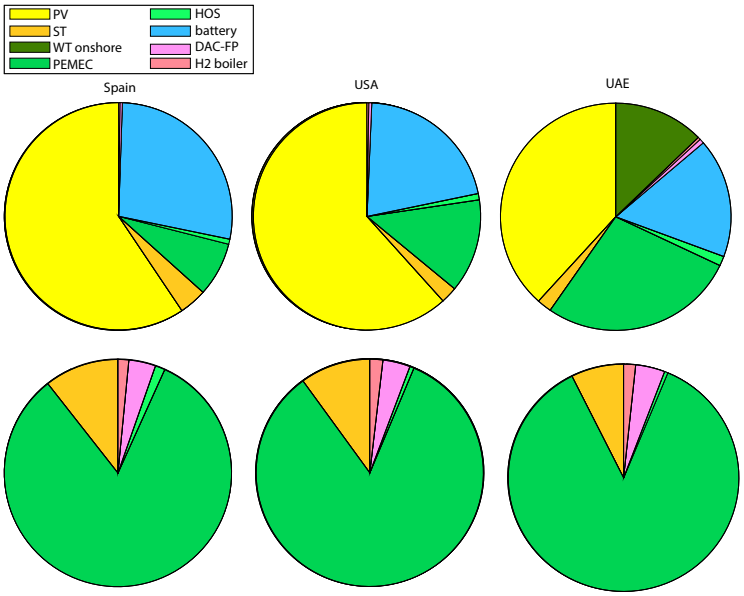

Figure A.1: Breakdown of the annualized costs associated to the autarkic (top) and network (bottom) system for the UU adsorption process for Spain, USA, and UAE.

Appendix B

Energy distribution

The energy flows and interactions between the technologies implemented in the optimal designs of the MES for Spain, USA, and UAE are presented. Similar patterns are observed between the different geographic locations. Explanation of the graphs is provided in Chapter 5.

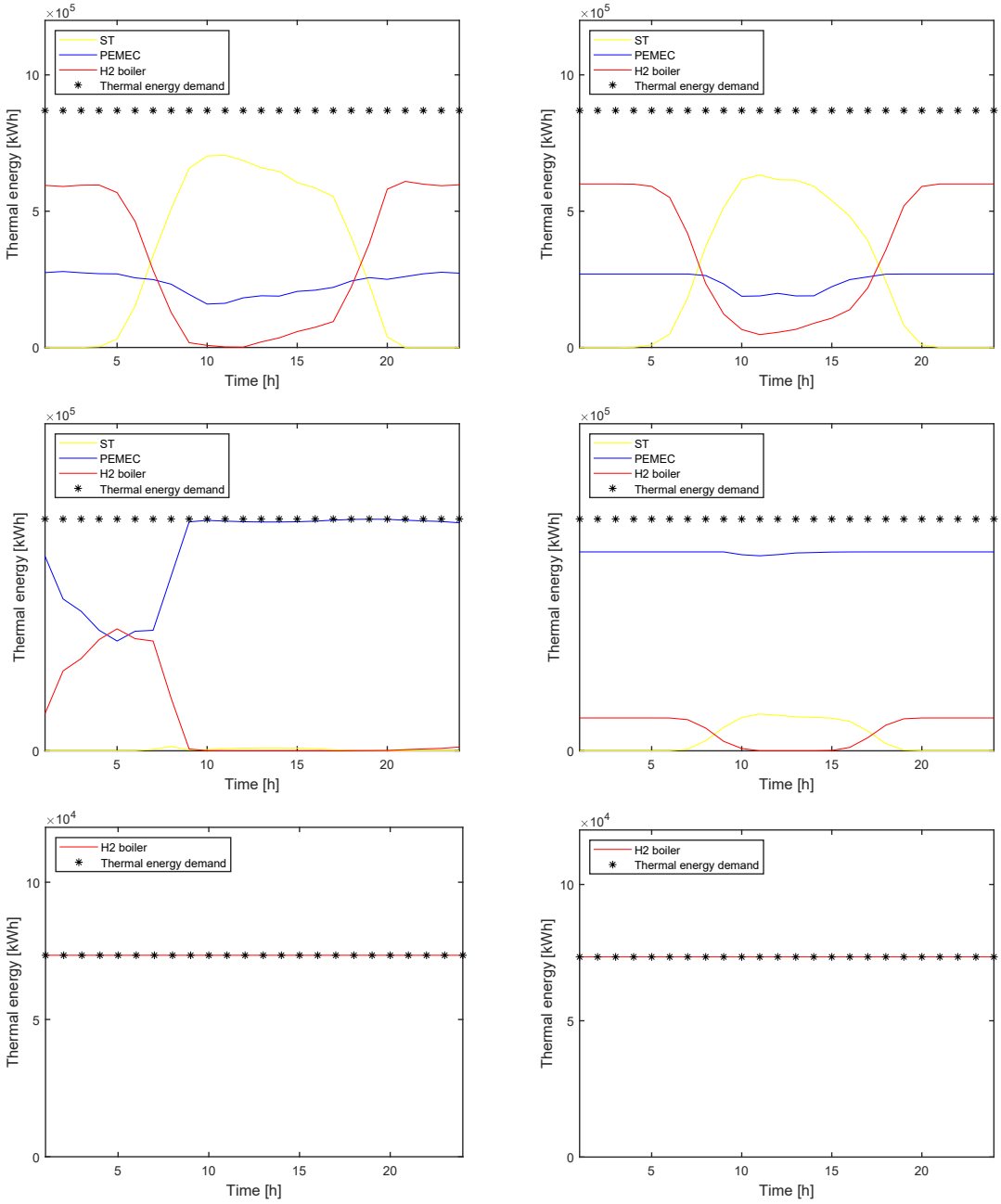

Figure B.1: Share of Spanish thermal energy sources. Top: autarky UU adsorption (left) and network UU adsorption (right). Middle: autarky CW adsorption (left) and network CW adsorption (right). Bottom: autarky CE absorption (left) and network CE absorption (right).

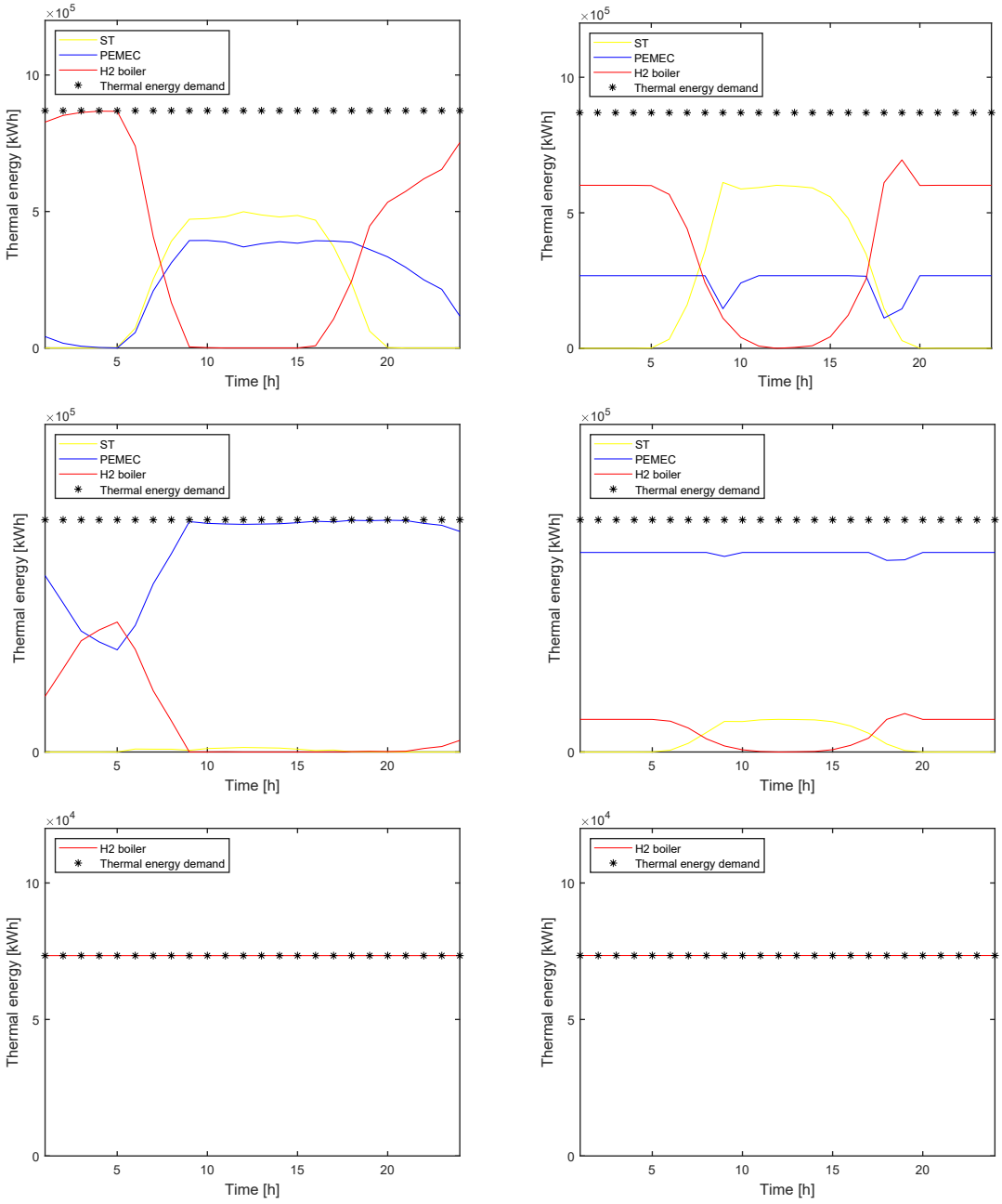

Figure B.2: Share of USA thermal energy sources. Top: autarky UU adsorption (left) and network UU adsorption (right). Middle: autarky CW adsorption (left) and network CW adsorption (right). Bottom: autarky CE absorption (left) and network CE absorption (right).

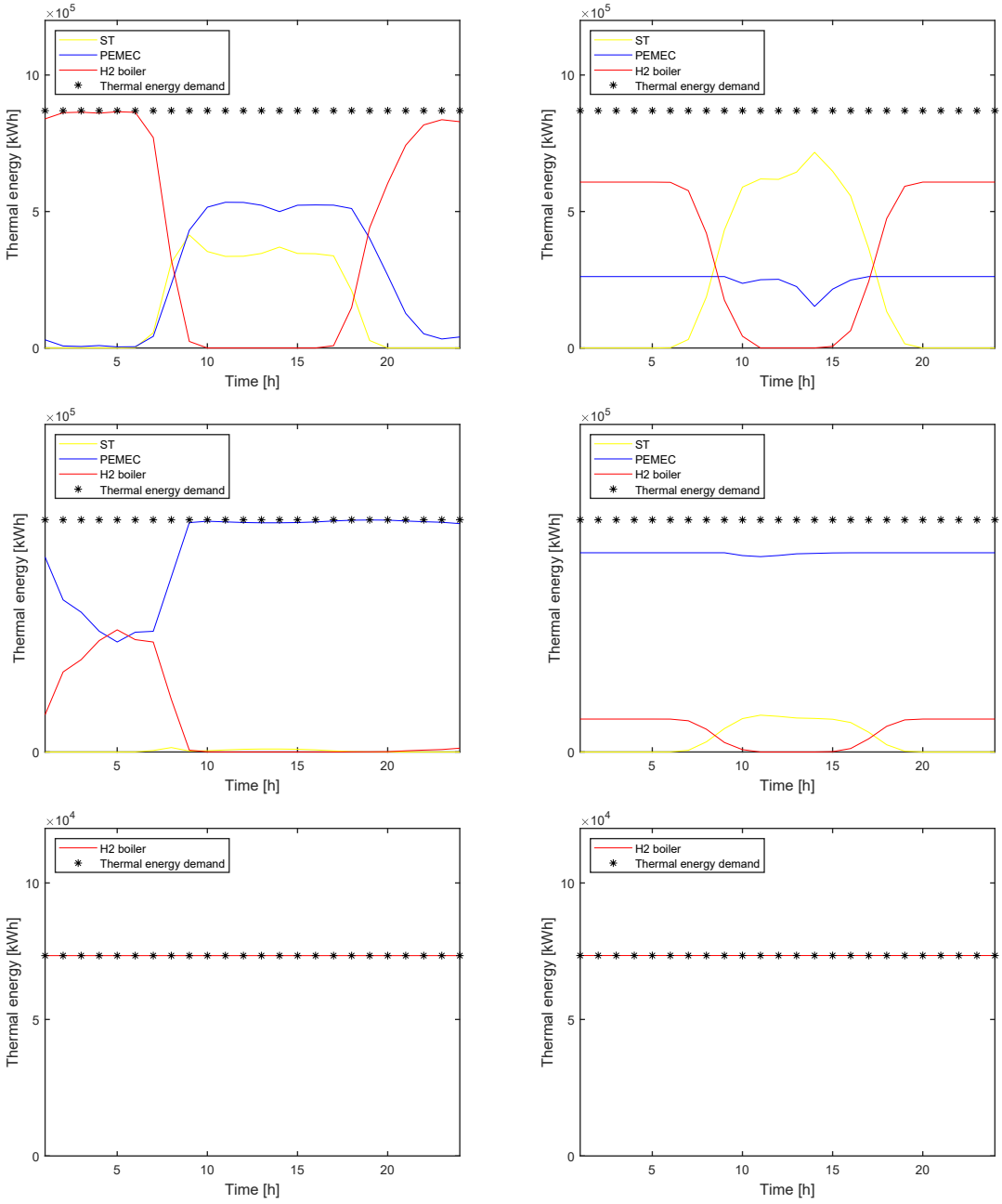

Figure B.3: Share of UAE thermal energy sources. Top: autarky UU adsorption (left) and network UU adsorption (right). Middle: autarky CW adsorption (left) and network CW adsorption (right). Bottom: autarky CE absorption (left) and network CE absorption (right).

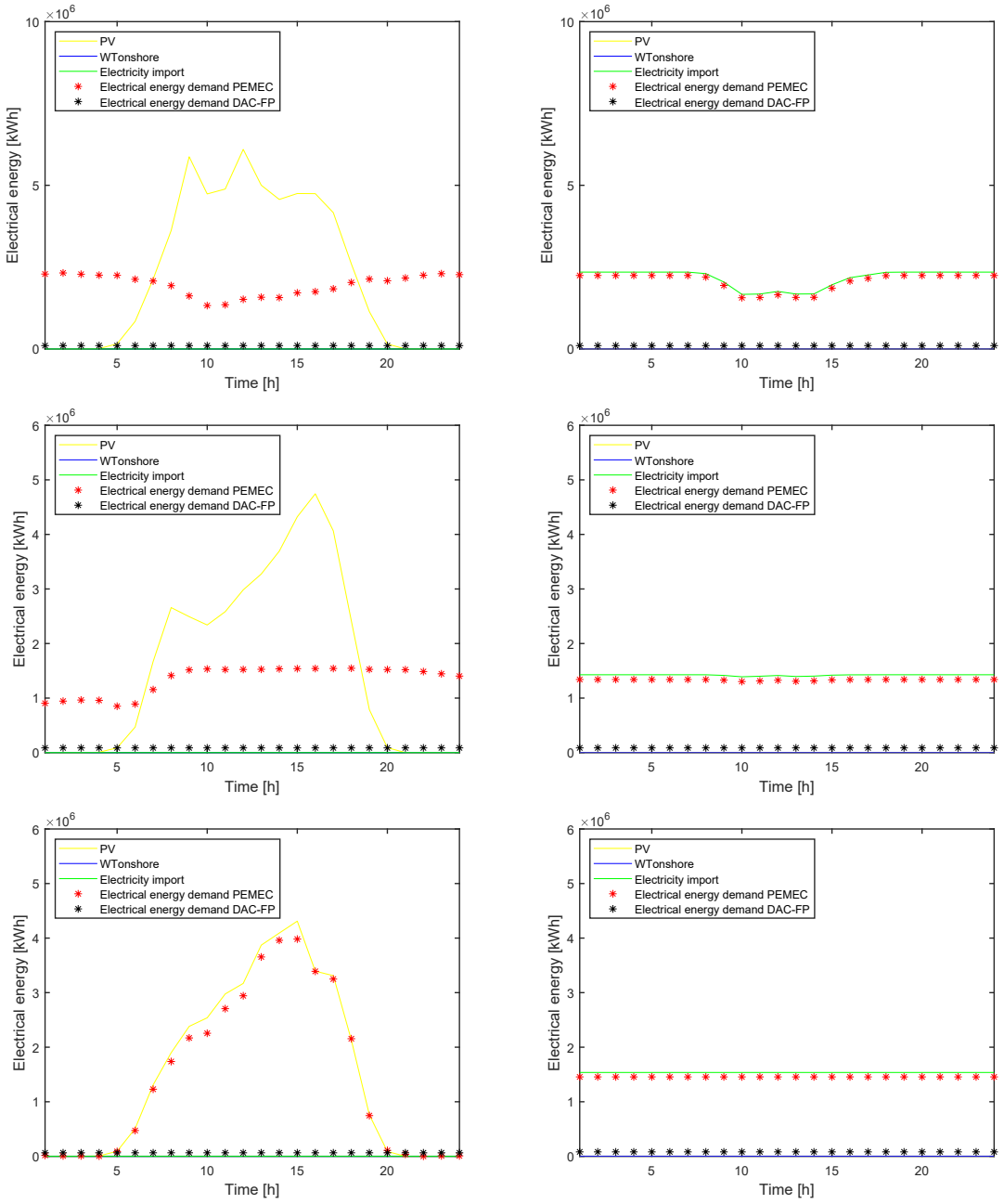

Figure B.4: Share of Spanish electrical energy sources. Top: autarky UU adsorption (left) and network UU adsorption (right). Middle: autarky CW adsorption (left) and network CW adsorption (right). Bottom: autarky CE absorption (left) and network CE absorption (right).

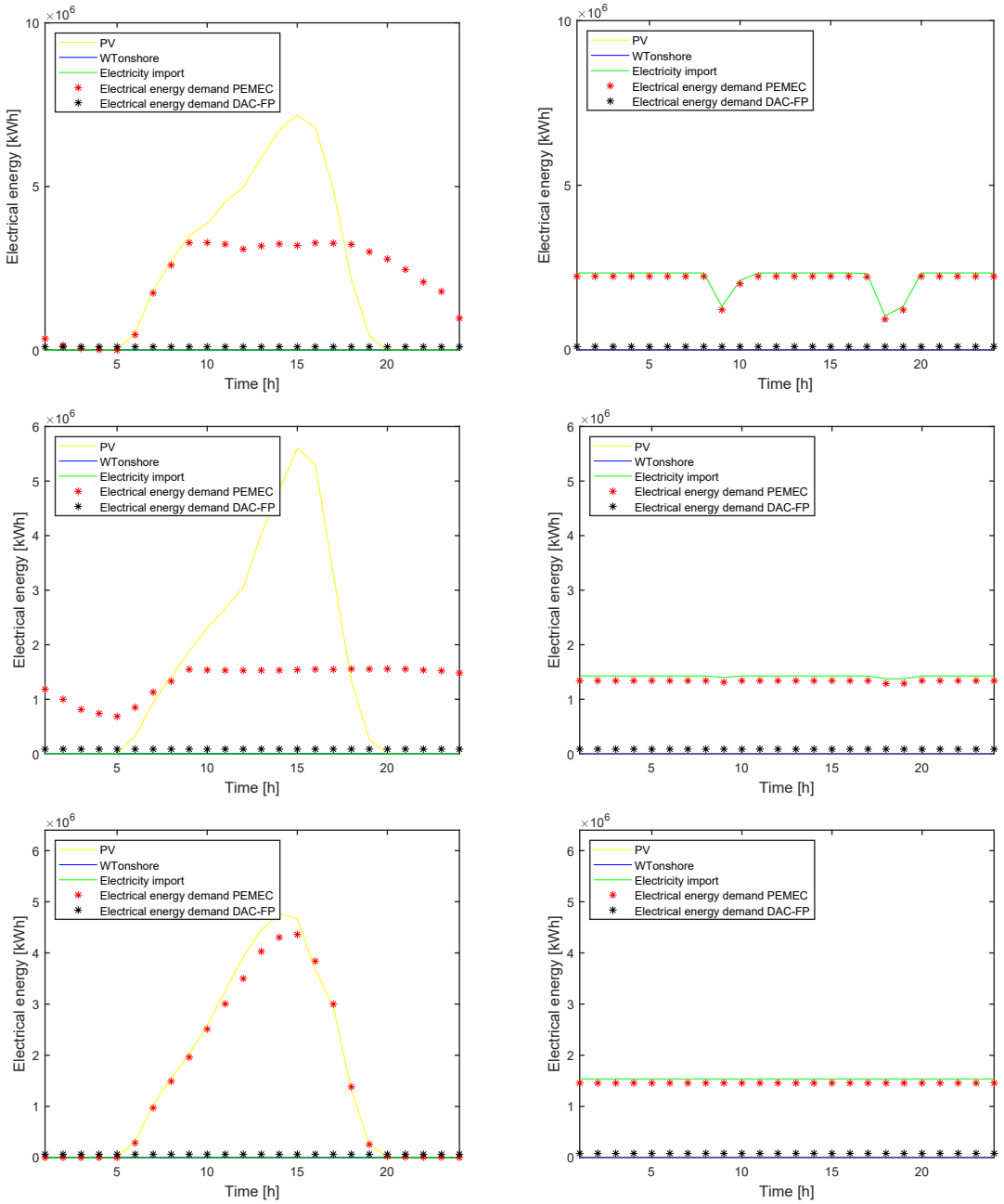

Figure B.5: Share of USA electrical energy sources. Top: autarky UU adsorption (left) and network UU adsorption (right). Middle: autarky CW adsorption (left) and network CW adsorption (right). Bottom: autarky CE absorption (left) and network CE absorption (right).

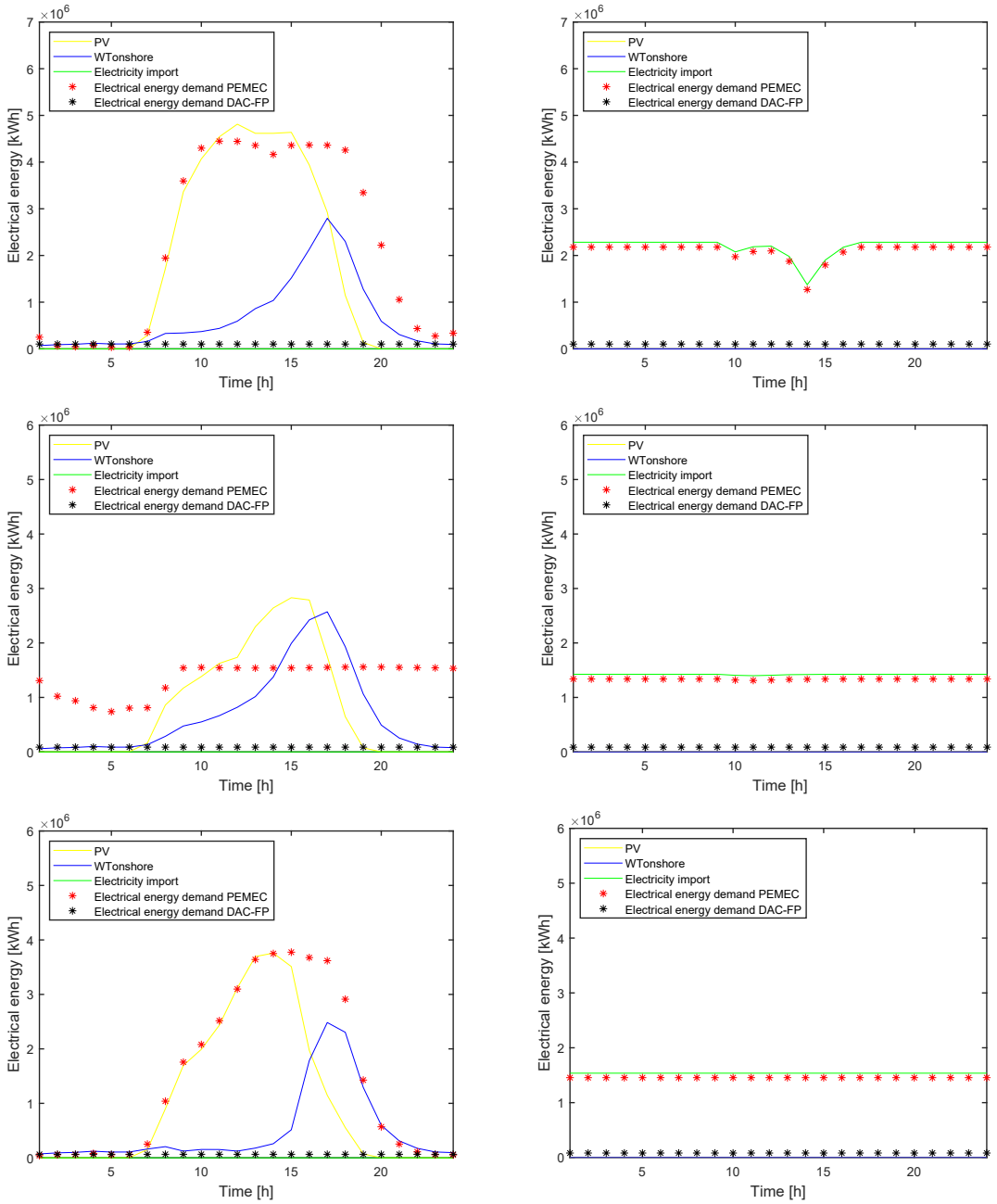

Figure B.6: Share of UAE electrical energy sources. Top: autarky UU adsorption (left) and network UU adsorption (right). Middle: autarky CW adsorption (left) and network CW adsorption (right). Bottom: autarky CE absorption (left) and network CE absorption (right).

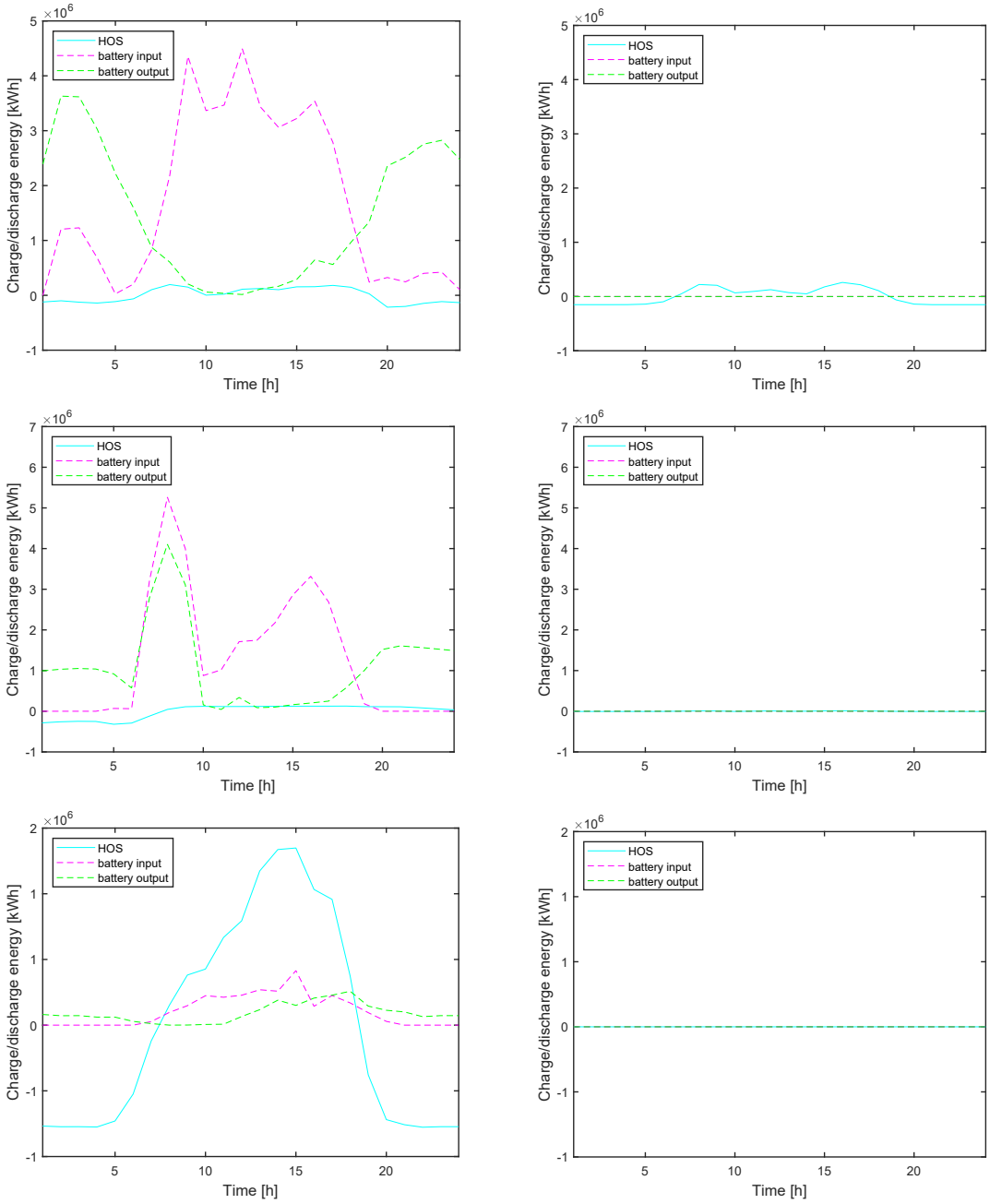

Figure B.7: Share of Spanish electrical energy storage and hydrogen storage. Top: autarky UU adsorption (left) and network UU adsorption (right). Middle: autarky CW adsorption (left) and network CW adsorption (right). Bottom: autarky CE absorption (left) and network CE absorption (right).

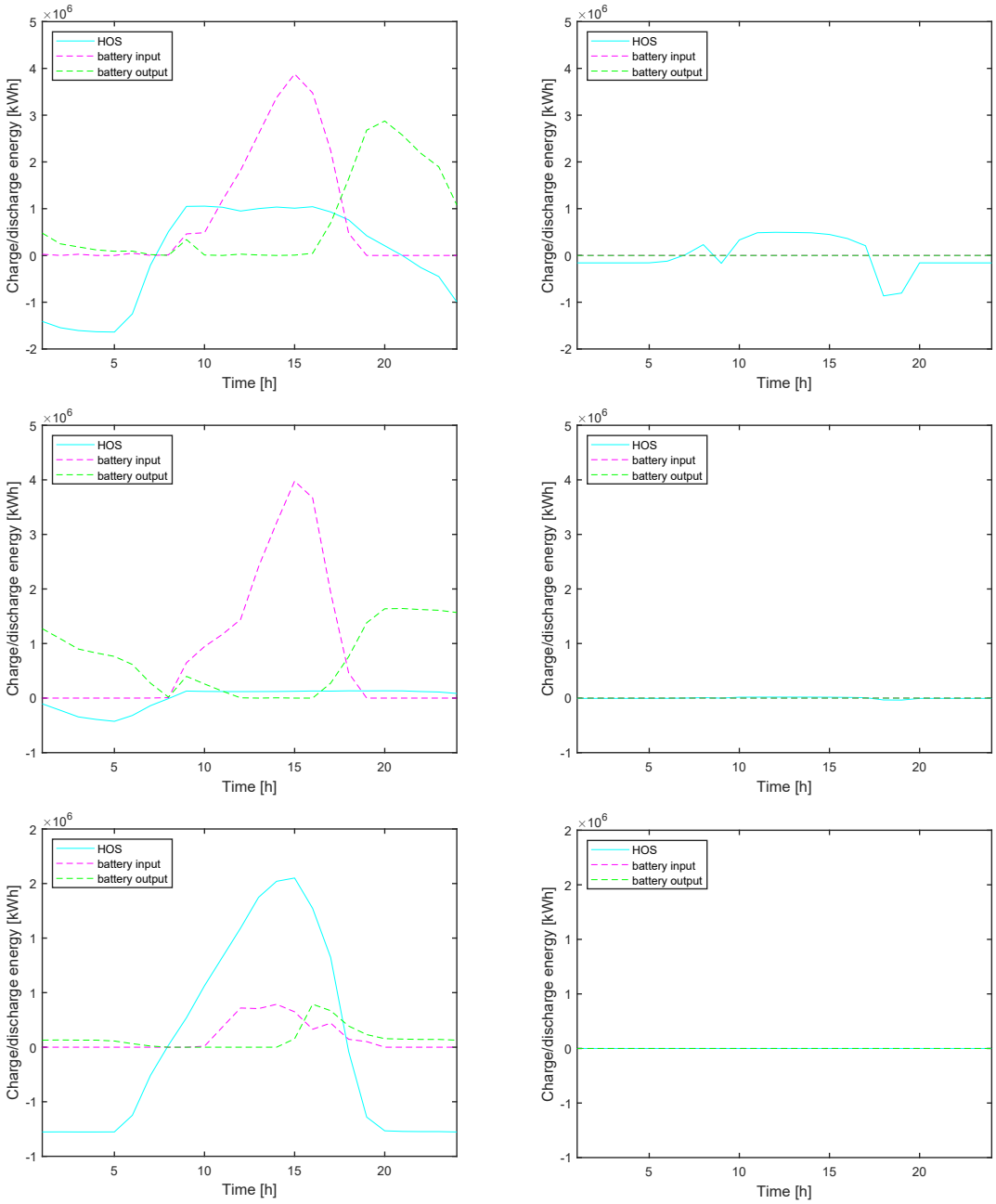

Figure B.8: Share of USA electrical energy storage and hydrogen storage. Top: autarky UU adsorption (left) and network UU adsorption (right). Middle: autarky CW adsorption (left) and network CW adsorption (right). Bottom: autarky CE absorption (left) and network CE absorption (right).

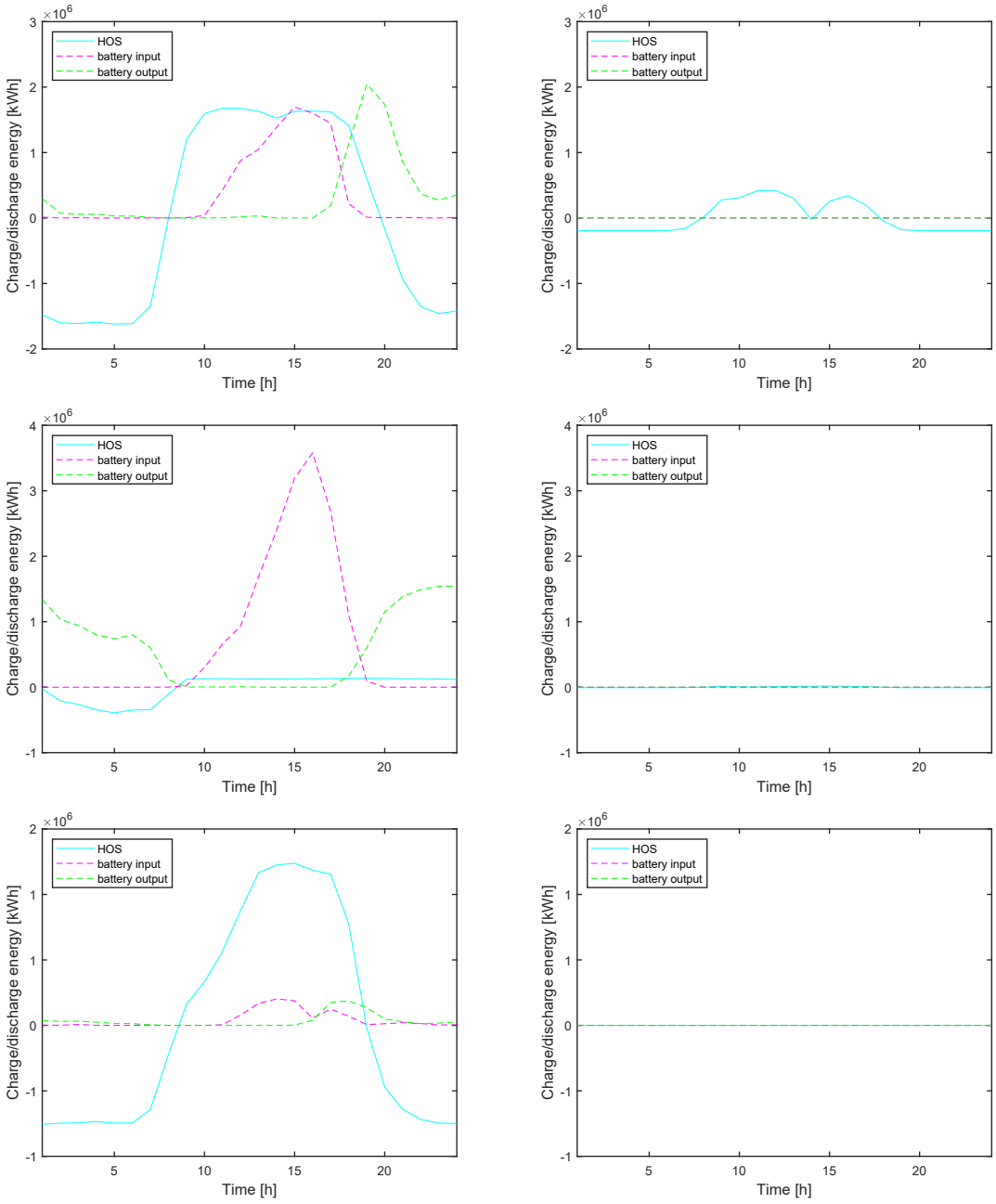

Figure B.9: Share of UAE electrical energy storage and hydrogen storage. Top: autarky UU adsorption (left) and network UU adsorption (right). Middle: autarky CW adsorption (left) and network CW adsorption (right). Bottom: autarky CE absorption (left) and network CE absorption (right).

Appendix C

Seasonal effects on energy storage

Countries with varying seasonal weather patterns, such as the Netherlands, experience difficulties coping with seasonal intermittency. Energy storage - both on electrochemical as electrical scale - needs to be implemented to overcome these difficulties. Large differences between winter and summer periods are observed (Figure C.1). Intensified fluctuations in summer periods are observed due to increase in renewable energy penetration.

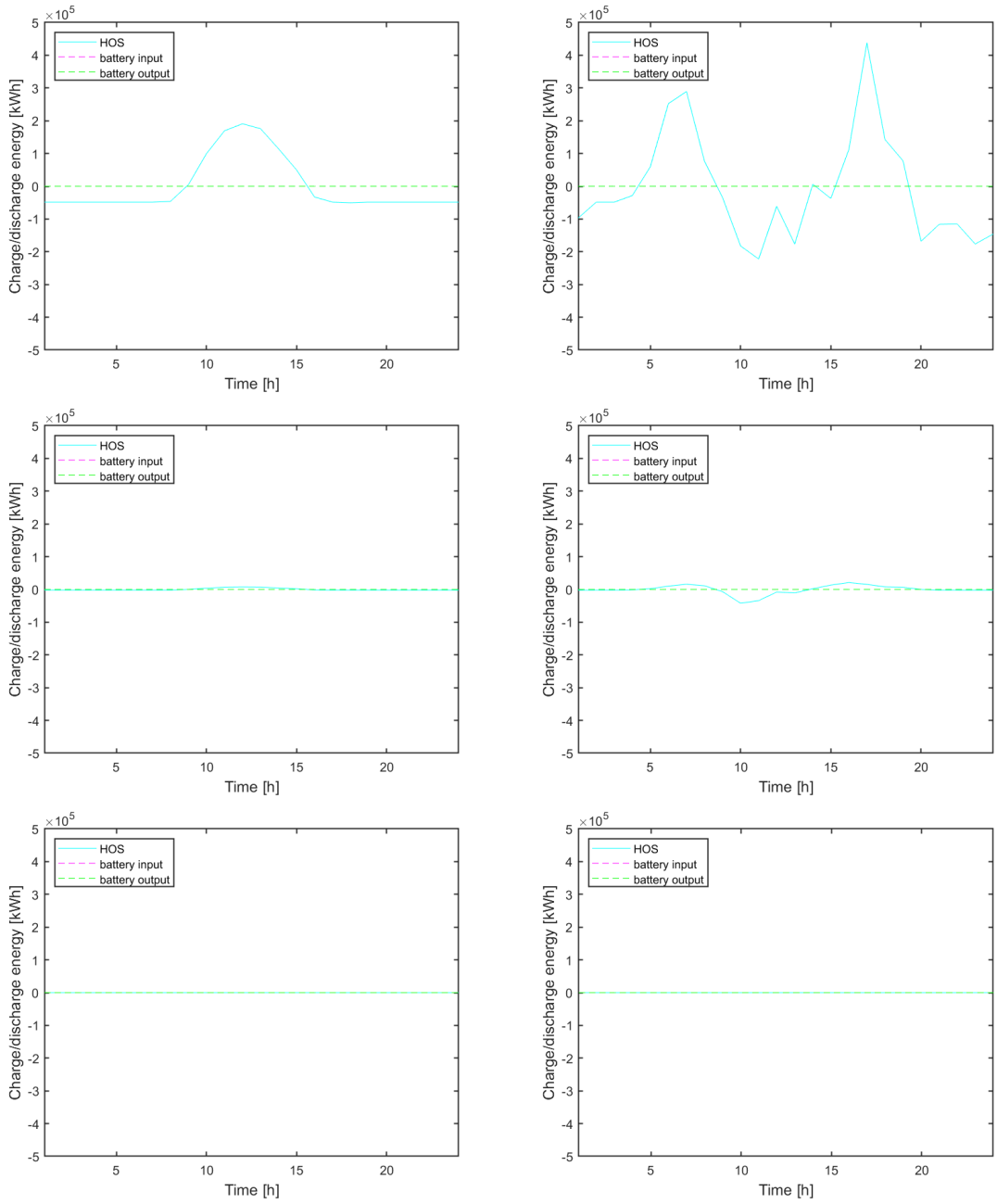

Figure C.1: Seasonal effects on Dutch network energy storage capacities. Top: winter UU adsorption (left) and summer UU adsorption (right). Middle: winter CW adsorption (left) and summer CW adsorption (right). Bottom: winter CE absorption (left) and summer CE absorption (right).

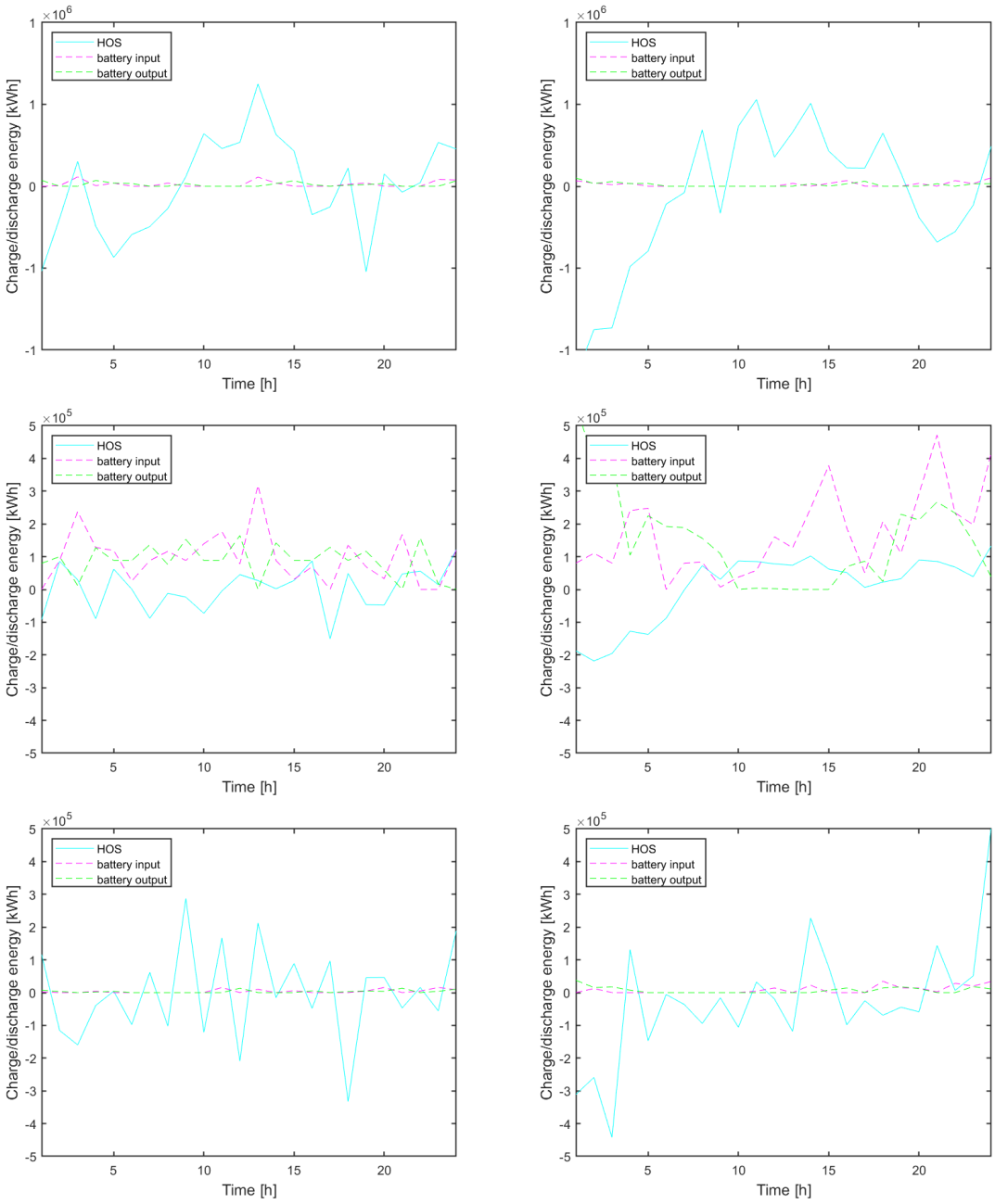

Figure C.2: Seasonal effects on Dutch autarkic energy storage capacities. Top: winter UU adsorption (left) and summer UU adsorption (right). Middle: winter CW adsorption (left) and summer CW adsorption (right). Bottom: winter CE absorption (left) and summer CE absorption (right).